Metabolism:

Transcriptional Regulatory Factor X6 (Rfx6) Increases Gastric Inhibitory Polypeptide (GIP) Expression in Enteroendocrine K-cells and Is Involved in GIP Hypersecretion in High Fat Diet-induced Obesity

Kazuyo Suzuki, Norio Harada, Shunsuke Yamane, Yasuhiko Nakamura, Kazuki Sasaki, Daniela Nasteska, Erina Joo, Kimitaka Shibue, Takanari Harada, Akihiro Hamasaki, Kentaro Toyoda, Kazuaki Nagashima and Nobuya Inagaki

J. Biol. Chem. 2013, 288:1929-1938.
doi: 10.1074/jbc.M112.423137 originally published online November 28, 2012

THE JOURNAL OF BIOLOGICAL CHEMISTRY VOL. 288, NO. 3, pp. 1929–1938, January 18, 2013

Transcriptional Regulatory Factor X6 (Rfx6) Increases Gastric Inhibitory Polypeptide (GIP) Expression in Enteroendocrine K-cells and Is Involved in GIP Hypersecretion in High Fat Diet-induced Obesity*

Received for publication, September 27, 2012, and in revised form, November 28, 2012 Published, JBC Papers in Press, November 28, 2012, DOI 10.1074/jbc.M112.423137

Kazuyo Suzuki, Norio Harada, Shunsuke Yamane, Yasuhiko Nakamura, Kazuki Sasaki, Daniela Nasteska, Erina Joo, Kimitaka Shibue, Takanari Harada, Akihiro Hamasaki, Kentaro Toyoda, Kazuaki Nagashima, and Nobuya Inagaki[1]

From the Department of Diabetes and Clinical Nutrition, Graduate School of Medicine, Kyoto University, 54 Kawahara-cho, Shogoin, Sakyo-ku, Kyoto 606-8507, Japan

Background: Gastric inhibitory polypeptide (GIP) secreted from enteroendocrine K-cells potentiates insulin secretion and induces energy accumulation into adipose tissue.
Results: Transcriptional Rfx6 is expressed in K-cells and increases GIP expression. Rfx6 expression is up-regulated in K-cells of obese mice.
Conclusion: Rfx6 plays critical roles in GIP expression and hypersecretion in obesity.
Significance: Gene analysis of K-cells isolated from GIP-GFP knock-in mice enabled identification of Rfx6.

Gastric inhibitory polypeptide (GIP) is an incretin released from enteroendocrine K-cells in response to nutrient ingestion. GIP potentiates glucose-stimulated insulin secretion and induces energy accumulation into adipose tissue, resulting in obesity. Plasma GIP levels are reported to be increased in the obese state. However, the molecular mechanisms of GIP secretion and high fat diet (HFD)-induced GIP hypersecretion remain unclear, primarily due to difficulties in separating K-cells from other intestinal epithelial cells *in vivo*. In this study, GIP-GFP knock-in mice that enable us to visualize K-cells by enhanced GFP were established. Microarray analysis of isolated K-cells from these mice revealed that transcriptional regulatory factor X6 (Rfx6) is expressed exclusively in K-cells. *In vitro* experiments using the mouse intestinal cell line STC-1 showed that knockdown of Rfx6 decreased mRNA expression, cellular content, and secretion of GIP. Rfx6 bound to the region in the *gip* promoter that regulates *gip* promoter activity, and overexpression of Rfx6 increased GIP mRNA expression. HFD induced obesity and GIP hypersecretion in GIP-GFP heterozygous mice *in vivo*. Immunohistochemical and flow cytometry analysis showed no significant difference in K-cell number between control fat diet-fed (CFD) and HFD-fed mice. However, GIP content in the upper small intestine and GIP mRNA expression in K-cells were significantly increased in HFD-fed mice compared with those in CFD-fed mice. Furthermore, expression levels of Rfx6 mRNA were increased in K-cells of HFD-fed mice. These results suggest that Rfx6 increases GIP expression and content in K-cells and is involved in GIP hypersecretion in HFD-induced obesity.

Obesity leads to insulin resistance characterized by fasting hyperinsulinemia and excessive insulin secretion to maintain euglycemia after meal ingestion (1). Obesity is an important risk factor in progression to type 2 diabetes mellitus (2) as well as cardiovascular disease (3), and reduction of obesity can normalize hyperinsulinemia and impede the progression of diabetes and arteriosclerosis.

Gastric inhibitory polypeptide, also called glucose-dependent insulinotropic polypeptide (GIP),[2] and glucagon-like peptide-1 (GLP-1) are the incretins, peptide hormones released from the gastrointestinal tract into circulation in response to meal ingestion that potentiate glucose-stimulated insulin secretion (4, 5). GIP is secreted from enteroendocrine K-cells located in the duodenum and upper small intestine; GLP-1 is secreted from enteroendocrine L-cells located in the lower small intestine and colon. GIP binds to the GIP receptor (GIPR) on the surface of pancreatic β-cells, adipose tissue, and osteoblasts, and it stimulates insulin secretion (6), fat accumulation (7), and bone formation (8), respectively, by increasing the level of intracellular adenosine 3′,5′-monophosphate (cAMP).

It was reported previously that GIPR-deficient mice exhibit insufficient compensatory insulin secretion upon high fat loading (9), suggesting that GIP plays a critical role in maintaining blood glucose levels by hypersecretion of insulin in diet-induced obesity. We also reported that sensitivity of GIPR to GIP in β-cells is increased in high fat diet (HFD)-induced obese mice (10). In addition, GIPR is expressed in adipose tissue (11) and increases glucose and triglyceride uptake in fat cells (12, 13). Thus, GIP has both direct and indirect effects on the accumulation of energy into adipose tissue. Some studies report that GIP secretion is increased in obesity (7, 14–16) and that pancreatic and duodenal homeobox 1 (Pdx1), which is known to be

* This work was supported by scientific research grants from the Ministry of Education, Culture, Sports, Science, and Technology, Japan, the Ministry of Health, Labor, and Welfare, Japan, and scientific research grants from the Japan Diabetes Foundation.
[1] To whom correspondence should be addressed. Tel.: 81-75-751-3562; Fax: 81-75-751-6601; E-mail: inagaki@metab.kuhp.kyoto-u.ac.jp.

[2] The abbreviations used are: GIP, gastric inhibitory polypeptide; GIPR, GIP receptor; HFD, high fat diet; CFD, control fat diet; EGFP, enhanced GFP; OGTT, oral glucose tolerance test.

an important transcription factor in pancreatic development and pancreatic β-cell maturation (17), has a critical role in GIP production in K-cells (18, 19). However, the mechanisms involved in GIP hypersecretion from K-cells in obesity remain unclear due to difficulties in separating these cells from other intestinal epithelial cells *in vivo*.

In this study, we investigated expression of various genes in K-cells by using GIP-GFP knock-in (GIP-GFP) mice in which K-cells can be visualized by EGFP fluorescence. We found that regulatory factor X6(Rfx6) is expressed exclusively in K-cells of the upper small intestine and is involved in GIP mRNA expression in the mouse small intestinal cell line STC-1. Furthermore, expression of Rfx6 as well as Pdx1 was found to be increased in K-cells of HFD-induced obese mice. Thus, GIP expression is stimulated by both Rfx6 and Pdx1, suggesting that these transcription factors play an important role in both GIP expression and GIP hypersecretion in HFD-induced obesity.

EXPERIMENTAL PROCEDURES

Animals—We designed targeting vector constructs as short-EGFP-poly(A)-loxp-Neo-loxp-long cassettes using mouse B6N BAC clone (identification numbers RP23-31E4 and RP23-383D10). A diphtheria toxin A expression cassette for negative selection was attached to the 3′ end of the *gip* sequence in the targeting vector. Next, the targeting vector was injected in embryonic stem cells from C57BL/6 mice, and a Neo resistance strain was established. The ES cells positive for the knock-in gene were selected by Southern blot analysis. The established ES cells were then injected into the blastocyst to obtain chimeric mice. Finally, we generated hetero-mutant mice by mating the chimeric mice with wild-type C57BL/6 mice. The mice were housed in an air-controlled (temperature 25 °C) room with a dark-light cycle of 10 and 14 h, respectively. Animal care and procedures were approved by the Animal Care Committee of Kyoto University.

GIP-GFP heterozygous mice (7 weeks of age) were fed control fat chow (CFD; 10% fat, 20% protein, and 70% carbohydrate by energy) or high fat chow (HFD; 60% fat, 20% protein, and 20% carbohydrate by energy) (Research Diets Inc., New Brunswick, NJ) for 8 weeks. Food intake, water intake, and body weight were measured.

Immunohistochemistry—Mouse upper small intestine samples were fixed in Bouin's solution and transferred into 70% ethanol before processing through paraffin. Rehydrated paraffin sections were incubated overnight at 4 °C with primary mouse anti-GFP antibody (sc-9996, 1:100, Santa Cruz Biotechnology) and rabbit anti-GIP antibody (T-4053, 1:100, Peninsula Laboratories, Inc., San Carlos, CA). Intestine samples and STC-1 cells (kindly provided by Prof. Hanahan, University of California, San Francisco) were embedded by Tissue-Tek O.C.T. compound 4583 (Sakura Fine Technical Co. Ltd., Tokyo, Japan) and immediately frozen in liquid nitrogen. Frozen sections (10 μm) on slides were air-dried and fixed in acetone for 5 min. Slides were then washed in phosphate-buffered saline (PBS) and blocked for 15 min in 3% BSA. They were incubated overnight at 4 °C with primary antibody (mouse anti-GIP antibody (1:100, kindly provided by Merck Millipore)) and goat anti-Rfx6 antibody (ABD28, 1:100, Merck). The sections were incubated for 1 h at room temperature with secondary antibody. Images were taken using a fluorescent microscopy with a BZ-8100 system (KEYENCE Corp., Osaka, Japan) and confocal microscopy with an LSM510META system (Carl Zeiss Co., Ltd., Jena, Germany).

Fifty representative mucous membranes from each slide were randomly selected, and their mean length and GFP-positive cells were quantified using fluorescent microscopy images. To count the GFP-positive cells, we distinguished the mucous membrane as villus, upper crypt, or lower crypt.

Isolation of K-cells from Mouse Intestinal Epithelium—Mouse upper small intestine was removed and washed by PBS. The intestine was cut into several round pieces and tied on one side with a thread. The pouch-like intestine was injected with Hanks' balanced salt solution containing 0.5 mg/ml collagenase, clamped, and incubated with CO_2 at 37 °C for 10 min in Krebs-Ringer bicarbonate buffer (KRBB: 120 mM NaCl, 4.7 mM KCl, 1.2 mM $MgSO_4$, 1.2 mM KH_2PO_4, 2.4 mM $CaCl_2$, 20 mM $NaHCO_3$). The digested intestinal epithelium was collected into the tube filled with Roswell Park Memorial Institute (RPMI) medium and rinsed twice. The intestinal epithelium was cultured in a humidified incubator (95% air and 5% CO_2) at 37 °C for 1 h. Afterward, it was centrifuged at 180 × *g* for 5 min, resuspended in PBS twice, and filtered with a cell strainer (352340, Falcon cell strainer, BD Biosciences). GFP-positive cells in the intestinal epithelium were analyzed using BD FACS Aria™ flow cytometer (BD Biosciences). Sorted cells were collected into vials containing medium at a rate of 2000 cells/tube.

Total RNA was extracted with PicoPure RNA isolation kit (Applied Biosystems, Inc., Alameda, CA) from sorted cells of GIP-GFP mouse intestinal epithelium and treated with DNase (Qiagen Inc., Valencia, CA). Microarray analysis was performed using GeneChip Mouse Genome 430 2.0 Array (Affymetrix Inc., Fremont, CA).

Glucose Tolerance Test (OGTT) and GIP Assay—After a 16-h fasting period, OGTTs (1 g/kg body weight) were performed. Blood samples were taken at the indicated times (0, 15, 30, 60, and 120 min after glucose loading), and blood glucose levels, plasma insulin levels, and plasma total GIP concentrations were measured. Blood glucose levels were determined by the glucose oxidase method (Sanwa Kagaku Kenkyusho Co. Ltd., Nagoya, Japan). Plasma insulin levels were determined using enzyme immunoassay (Shibayagi, Gumma, Japan). Plasma total GIP levels were determined using an ELISA kit (Merck Millipore).

For measurement of GIP content in the mouse upper small intestine, the mice were killed at 15 weeks of age after 8 weeks of CFD or HFD feeding. The intestine was rapidly removed and washed in PBS. After measuring the weight, samples were extracted with 5 ml/g acid ethanol, and GIP levels were measured (15).

Quantitative RT-PCR—Complementary DNA (cDNA) was prepared by reverse transcriptase (Invitrogen) with an oligo(dT) primer (Invitrogen). Messenger RNA (mRNA) levels were measured by quantitative RT-PCR using ABI PRISM 7000 Sequence Detection System (Applied Biosystems Inc.). PCR analyses were carried out using the oligonucleotide primers. SYBR Green PCR master mix (Applied Biosystems Inc.) was prepared for PCR run. Thermal cycling conditions were dena-

turation at 95 °C for 10 min followed by 50 cycles at 95 °C for 15 s and 60 °C for 1 min. C- and N-terminal primers of target molecules were designed as follows: GIP forward, 5′-gtggctttgaagacctgctc-3′, and reverse, 5′-ttgttgtcggatcttgtcca-3′; GFP forward, 5′-gtggctttgaagacctgctc-3′, and reverse, 5′-tttacgtcgccgtccagctcg-3′; GLP-1 forward, 5′-tgaagacaaacgccactcac-3′, and reverse, 5′-tcatgacgtttggcaatgtt-3′; Pdx1 forward, 5′-gacctttcccgaatggaa-3, and reverse, 5′-cttgttttcctcgggttc-3′; Rfx1 forward, 5′-gcagccagaagcagtatgtg-3′, and reverse, 5′-tggcttctgacacagtctcact-3′; Rfx2 forward, 5′-cagaactccgagggaggag-3′, and reverse, 5′-ggagggtgagtgtctgcatc-3′; Rfx3 forward, 5′-cgtcacaggaggacaactca-3′, and reverse, 5′-cagacttttgcagcgtctca-3′; Rfx4 forward, 5′-ccgaatacactggccttagc-3′, and reverse, 5′-atgggtgctcctcatacagg-3′; Rfx5 forward, 5′-tctaccttcagctccatcg-3′, and reverse, 5′-ggcaggtatccatgtgctct-3′; Rfx6 forward, 5′-acagacacggaatctgacat-3′, and reverse, 5′-ctctaccacagtgtccaacc-3′; Rfx7 forward, 5′-cgctctgcaacacaagatca-3′, and reverse, 5′-gaccagaaggcagttgaagg-3′; and GAPDH forward, 5′-aaatggtgaaggtcggtgtg-3′, and reverse, 5′-tcgttgatggcaacaatctc-3′.

Cell Culture and Small Interfering RNA (siRNA) Transfection into STC-1 Cells—STC-1 cells, mouse small intestinal cell line, were cultured in Dulbecco's modified Eagle's medium (DMEM) (Sigma) supplemented with 10% heat-inactivated fetal calf serum, 100 IU/ml penicillin, and 100 μg/ml streptomycin at 37 °C in a humidified atmosphere (5% CO_2 and 95% air). siRNA transfection of Stealth™ siRNAs were synthesized (Invitrogen). The sequences of siRNAs specific for Rfx6 and Pdx1 are shown as follows: Pdx1, caguacuacgcggccacacagcucu and agagcuguguggccgcguaguacug, and Rfx6, ggugaaugccaugguaucugauauu and aauaucagauaccauggcauucacc. Cultured STC-1 cells were trypsinized, suspended with DMEM without antibiotics, mixed with Opti-MEM (Invitrogen) containing siRNA and Lipofectamine TM2000 (Invitrogen), plated on 12-well dishes, and then incubated at 37 °C in a CO_2 incubator. The amounts of STC-1 cells were 1×10^6 cells/well. Medium was replaced with 1 ml of DMEM containing antibiotics about 5–6 h after transfection. RT-PCR was performed 48 h after transfection.

Plasmid Construction and Transfection into STC-1 Cells—The cDNA fragment of mouse Rfx6 protein was obtained from mouse (C57BL/6) islets by RT-PCR. The cDNA fragment of Rfx6 was cloned into pCMV vector (Clontech). Expression plasmids of Rfx6 cDNA were transfected into STC-1 cells using Lipofectamine™ 2000 (Invitrogen). Plasmid (8 μg/well) was diluted into Opti-MEM, and Lipofectamine™ 2000 was added and incubated at room temperature for 20 min. After incubation, the mixture was added to STC-1 cells (1×10^6 cells/well). RT-PCR was performed 48 h after transfection.

Measurement of Incretin Release and Cellular Content in STC-1 Cells—For incretin release assays, DMEM was collected from STC-1 cells cultured on 12-well dishes about 42–43 h after changing the medium (48 h after transfection). Media were centrifuged at 3000 × *g* for 10 min, and the supernatant was collected. Total GIP and total GLP-1 levels were measured by ELISA methods (Merck Millipore and Meso Scale Discovery (Gaithersburg, MD), respectively) as incretin release from STC-1 cells.

To determine incretin content, STC-1 cells cultured on 12-well dishes (48 h after transfection) were washed with PBS and homogenized in 0.5 ml of 0.1 N HCl and extracted at RT for 10 min, after which the supernatant was collected and centrifuged at 3000 × *g* for 10 min. Incretin and protein levels were measured by ELISA (GIP and GLP-1) and Bradford reagent (Bio-Rad), respectively.

Yeast One-hybrid Assay—Yeast one-hybrid assays were performed using the Matchmaker Gold Yeast One-hybrid Library Screening System (Clontech) according to the manufacturer's protocol. The *gip* promoter fragments shown in Fig. 4*A* were inserted separately upstream of the aureobasidin A resistance gene on the pAbAi vector, and Rfx6 cDNA was inserted downstream of GAL4-activating domain (GAL4AD) on the pGADT7 activating domain vector. The interactions between *gip* promoter fragments and Rfx6-GAL4AD protein were assayed using the aureobasidin A resistance gene reporter system. First, *Saccharomyces cerevisiae* Y1HGold (*MATα, ura3-52, his3-200, ade2-101, trp1-901, leu2-3, 112, gal4Δ, gal80Δ, met-MEL1*) was transformed by *gip* promoter fragment-inserted pAbAi plasmid (pAbAi-fragments a, b, c, and d), and spread on the synthetic medium with dextrose (SD) (without uracil) and incubated for 1 week at 30 °C. Obtained yeast was transformed by Rfx6 cDNA-inserted pGADT7 activating domain plasmid (pGADT7-Rfx6), spread on the SD (without tryptophan) medium, and then incubated for 1 week at 30 °C. Interaction between *gip* promoter fragment and Rfx6-GAL4AD protein could be detected, and the transformant was grown on SD (without tryptophan) medium containing 600 ng/ml aureobasidin A.

GIP Promoter Activity—1×10^6 STC-1 cells were cotransfected with pGL4.19 luciferase reporter plasmid expressing five different lengths of the *gip* promoter gene (Fig. 4*C*) and pGL4.73 *Renilla* luciferase reporter plasmid. 48 h after transfection, luciferase and *Renilla* activities were assayed according to the manufacturer's protocol (Promega Corp., Madison, WI) using a GioMax 20/20n luminometer (Promega). Firefly luciferase activity was normalized to *Renilla* luciferase expression and is presented as fold increase in relative light units over samples transfected with pGL4.19. All samples were analyzed in duplicate.

Analysis—The results are given as means ± S.E. (S.E., n = number of mice). Statistical significance was determined using paired and unpaired Student's t test and analysis of variance. $p \leq 0.05$ was considered significant.

RESULTS

Visualization and Isolation of K-cells Using GIP-GFP Mice—GIP-GFP mice were generated for the purpose of visualizing enteroendocrine K-cells (Fig. 1*A*). The mouse *gip* gene is composed of six exons. The targeting vector for GIP-GFP mice was designed so that EGFP cDNA was fused with exon 3 in the *gip* gene. Prepro-GIP consists of 144 amino acids (Fig. 1*B*), and PC1/3 and PC2 cleave prepro-GIP, generating GIP(1–42) and GIP(1–30), respectively. In GIP-GFP mice, the fusion protein retains the signal peptide, but it does not have the GIP(1–42) sequence nor the PC1/3 and PC2 cleavage sites. Accordingly, GIP-GFP mice express GIP signal peptide-GFP fusion protein

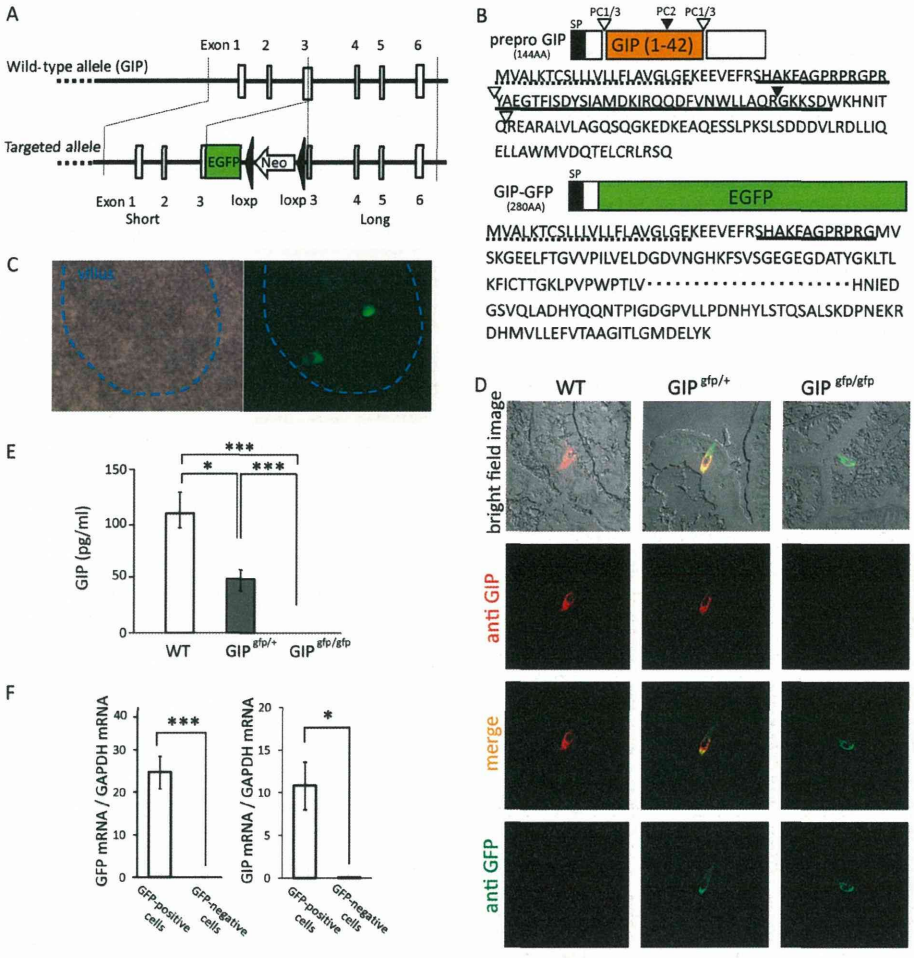

FIGURE 1. **Gene construct of GIP-GFP mice.** *A,* wild-type GIP allele and targeted allele of GIP-GFP. EGFP-poly(A)-loxp-Neo-loxp cassette was inserted into exon 3 of wild-type *gip* gene. *B,* prepro-GIP protein and GIP-GFP fusion protein. *SP,* signal peptide. *Open triangle,* PC1/3 cleavage site; *closed triangle,* PC2 cleavage site; *dotted line,* amino acids of signal peptide; *solid line,* translated protein from exon 3. *C,* microscopic images of upper small intestine in GIP-GFP heterozygous mice (bright field image and fluorescence image). *D,* immunohistochemical images of upper small intestine in wild-type (*WT*), GIP-GFP heterozygous ($GIP^{gfp/+}$), and homozygous mice ($GIP^{gfp/gfp}$). *Green,* GFP-expressing cells; *red,* GIP-expressing cells; *yellow,* merged image. *E,* fasting plasma GIP levels in WT, $GIP^{gfp/+}$, and $GIP^{gfp/gfp}$ mice. *F,* GFP mRNA and GIP mRNA levels in GFP-positive cells ($n = 5–6$) and GFP-negative cells ($n = 5–6$). *, $p \leq 0.05$; **, $p \leq 0.01$; ***, $p \leq 0.001$.

(280 amino acids). GFP fluorescence was observed in the small intestine of GIP-GFP heterozygous mice (Fig. 1*C*) and GIP-GFP homozygous mice (data not shown).

Immunohistochemical analysis was performed to assess localization of GFP-expressing cells and GIP-expressing cells using anti-GFP and anti-GIP antibodies, respectively, in the upper small intestine of wild-type and GIP-GFP heterozygous and homozygous mice (Fig. 1*D*). GFP-expressing cells are present in the intestine of GIP-GFP heterozygous and homozygous mice and GIP-expressing cells are present in the intestine of both wild-type and GIP-GFP heterozygous mice. However, in GIP-GFP homozygous mice, no GIP-expressing cells were found. The GFP-expressing cells were identical to the GIP-expressing cells in the GIP-GFP heterozygous mice. We then examined the fasting plasma GIP levels in the three types of mice (Fig. 1*E*). GIP levels were significantly lower in GFP-GFP heterozygous mice compared with those in wild-type mice. GIP levels of GIP-GFP homozygous mice were not detectable. These results indicate that GIP-GFP heterozygous mice have only one normal *gip* gene and that GIP-GFP homozygous mice have no normal *gip* genes.

Next, GFP-positive cells were purified by a flow cytometry system. GFP-positive cells and GFP-negative cells from upper small intestinal epithelium of GIP-GFP heterozygous mice were separated and collected. GFP mRNA and GIP mRNA were highly expressed in GFP-positive cells (Fig. 1*F*). In microarray analysis, the expression levels of GIP mRNA were much higher in GFP-positive cells than those in GFP-negative cells (GFP-positive cells ($n = 3$) 12,951.55 ± 335.77 *versus* GFP-negative cells ($n = 3$) 1763.61 ±142.65; $p \leq 0.001$). These results demonstrate that the GFP-positive cells in the intestinal epithelium of GIP-GFP mice are K-cells.

Transcription Factor Rfx6 Is Expressed Exclusively in K-cells—Microarray analysis data revealed that mRNA of the transcription factor Rfx6 is highly expressed in GFP-positive cells (GFP-positive cells ($n = 3$) 2613.4 ± 341.9 *versus* GFP-negative cells ($n = 3$) 24.0 ± 6.7; $p \leq 0.05$). As seven members of the Rfx family were identified previously, we evaluated the expression

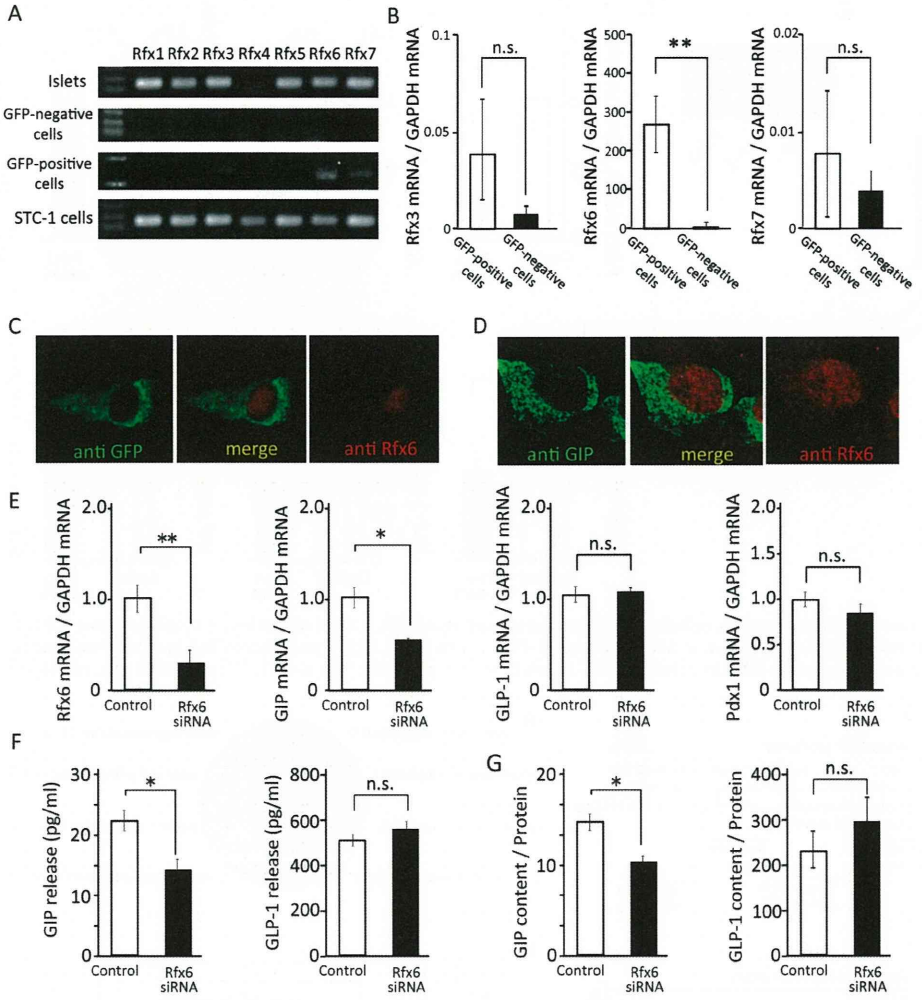

FIGURE 2. **Effect of Rfx6 on mRNA expression, cellular content, and secretion of GIP in STC-1 cells.** *A,* mRNA expression for *rfx* genes 1–7 in islets, GFP-negative cells, GFP-positive cells, and STC-1 cells by PCR. *B,* Rfx3, Rfx6, and Rfx7 mRNA levels in GFP-positive cells (n = 8–10) and GFP-negative cells (n = 8–10). *C,* immunohistochemical images of upper small intestine in GIP-GFP heterozygous mice. *Green,* GFP-expressing cells; *red,* Rfx6-expressing cells; *yellow,* merged image. *D,* immunohistochemical images of STC-1 cells. *Green,* GIP-expressing cells; *red,* Rfx6-expressing cells; *yellow,* merged image. *E,* Rfx6, GIP, GLP-1, and Pdx1 mRNA levels in Rfx6 knockdown STC-1 cells (n = 4). *F* and *G,* incretin content and secretion in Rfx6 knockdown STC-1 cells (n = 4). *, $p \leq 0.05$; **, $p \leq 0.01$, *n.s.*, not significant.

of these mRNAs in mouse islets, GFP-positive cells (K-cells), and mouse small intestinal cell line STC-1 (Fig. 2*A*). All of the *rfx* genes, except for *rfx4*, were expressed in islets as shown in a previous study (20). Rfx3, Rfx6, and Rfx7 were expressed in GFP-positive cells, but no Rfx mRNAs were detected in the GFP-negative cells. In semi-quantitative RT-PCR data, the expression levels of Rfx6 were extremely higher in GFP-positive cells than those in GFP-negative cells, whereas the expression levels of Rfx3 and Rfx7 were similar (Fig. 2*B*). Immunohistochemistry confirmed that Rfx6-expressing cells correspond to GFP-expressing cells (Fig. 2*C*), demonstrating that Rfx6 is expressed exclusively in K-cells.

Inhibition of Rfx6 and Pdx1 Expression Decreases GIP Expression in STC-1 Cells—We then assessed the influence of Rfx6 on GIP expression and secretion by using STC-1 cells. Rfx6 mRNA expression was confirmed in STC-1 cells by RT-PCR (Fig. 2*A*). The Rfx6-expressing cells were similarly located in the GIP-expressing cells by immunohistochemistry (Fig. 2*D*). By treatment with Rfx6 siRNA, Rfx6 mRNA expression was inhibited by 70% (Fig. 2*E*). In the same condition, mRNA expression, cellular content, and secretion of GIP were significantly decreased whereas those of GLP-1 were similar to control (Fig. 2, *E–G*), indicating that Rfx6 increases GIP mRNA expression, cellular content, and secretion. However, Pdx1 is reported to be an important transcriptional factor for producing GIP in K-cells (17, 18), although its expression levels were similar in GFP-positive and GFP-negative cells (Fig. 3*A*). To examine the effect of Pdx1 on incretin expression and secretion, mRNA expression, cellular content, and secretion of GIP and GLP-1 were measured in Pdx1-knockdown STC-1 cells by using siRNA. Pdx1 mRNA expression was confirmed in STC-1 cells by RT-PCR (Fig. 3*B*). The expression levels of Pdx1 mRNA were decreased by 50% in STC-1 cells treated with Pdx1 siRNA (Fig. 3*C*). GIP mRNA expression, cellular content, and secretion were significantly decreased, whereas GLP-1 mRNA expression, cellular content, and secretion were somewhat increased in STC-1 cells treated with Pdx1 siRNA (Fig. 3, *C–E*). The expression levels of Rfx6 mRNA were significantly decreased in the cells (Fig. 3*C*).

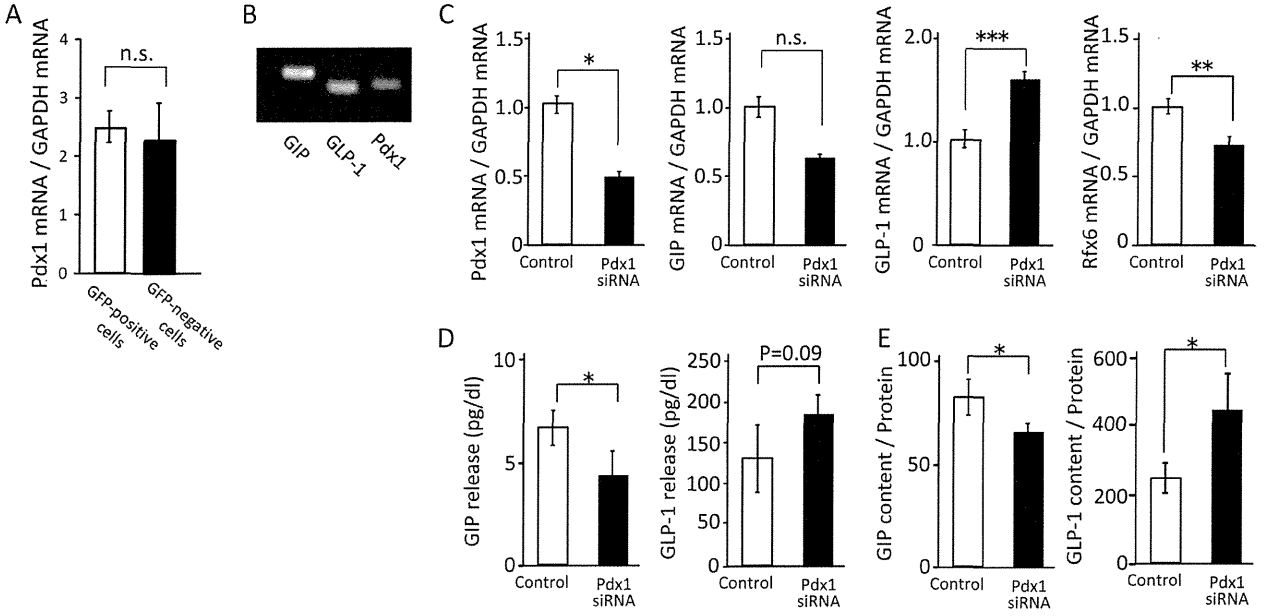

FIGURE 3. **Effect of Pdx1 on mRNA expression, cellular content, and secretion of GIP.** *A*, Pdx1 mRNA levels in GFP-positive cells and GFP-negative cells (n = 8–10). *B*, GIP, GLP-1, and Pdx1 mRNA expressions in STC-1 cells by RT-PCR. *C*, Pdx1, GIP, GLP-1, and Rfx6 mRNA levels in Pdx1 knockdown STC-1 cells (n = 4). *D* and *E*, incretin content and secretion in Pdx1 knockdown STC-1 cells (n = 4). *, $p \leq 0.05$; **, $p \leq 0.01$; ***, $p < 0.001$, *n.s.*, not significant.

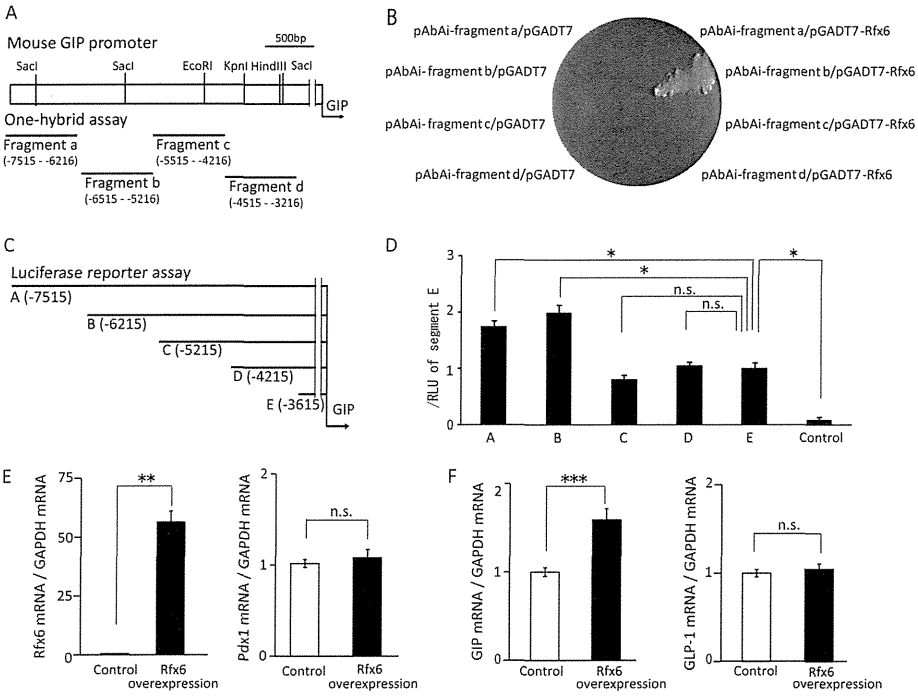

FIGURE 4. **Interaction of Rfx6 and *gip* gene.** *A*, design of the *gip* promoter fragments for one-hybrid assay. *Numbers* indicate nucleotides upstream from the transcription start site of the *gip* gene. *B*, results of yeast one-hybrid assay. Only yeast transformed with both pAbAi vector containing fragment b (*pAbAi-fragment b*) and Rfx6 cDNA-inserted pGADT7 (*pGADT7-Rfx6*) was grown on SD medium. *C*, design of the different lengths of *gip* promoter genes for luciferase reporter plasmid transfected in STC-1 cells. *D*, luciferase promoter assay on *gip* promoter. Data are represented by ratio of relative light units (*RLU*) of fragment E (n = 3–4). *, $p \leq 0.05$, *n.s.*, not significant. *E* and *F*, Pdx1, Rfx6, GIP, and GLP-1 mRNA levels in Rfx6-overexpressing STC-1 cells. **, $p \leq 0.01$; ***, $p \leq 0.001$ *versus* control, *n.s.*, not significant.

Interaction of Rfx6 and GIP Gene—We assessed the interaction of the Rfx6 and *gip* gene by one-hybrid assay. Four fragments of the *gip* promoter were constructed (Fig. 4*A*). Rfx6 effectively bound to fragment b (5216–6512 base pairs (bp) upstream of the *gip* promoter) (Fig. 4*B*). In the luciferase promoter assay, *gip* promoter activity of fragments A and B containing 5216–6512 bp upstream of *gip* promoter was high, whereas the activities of *gip* promoter C, D, and E were significantly decreased (Fig. 4*D*). These results suggest that Rfx6 binds to the region 5216–6512 bp upstream of the *gip* promoter,

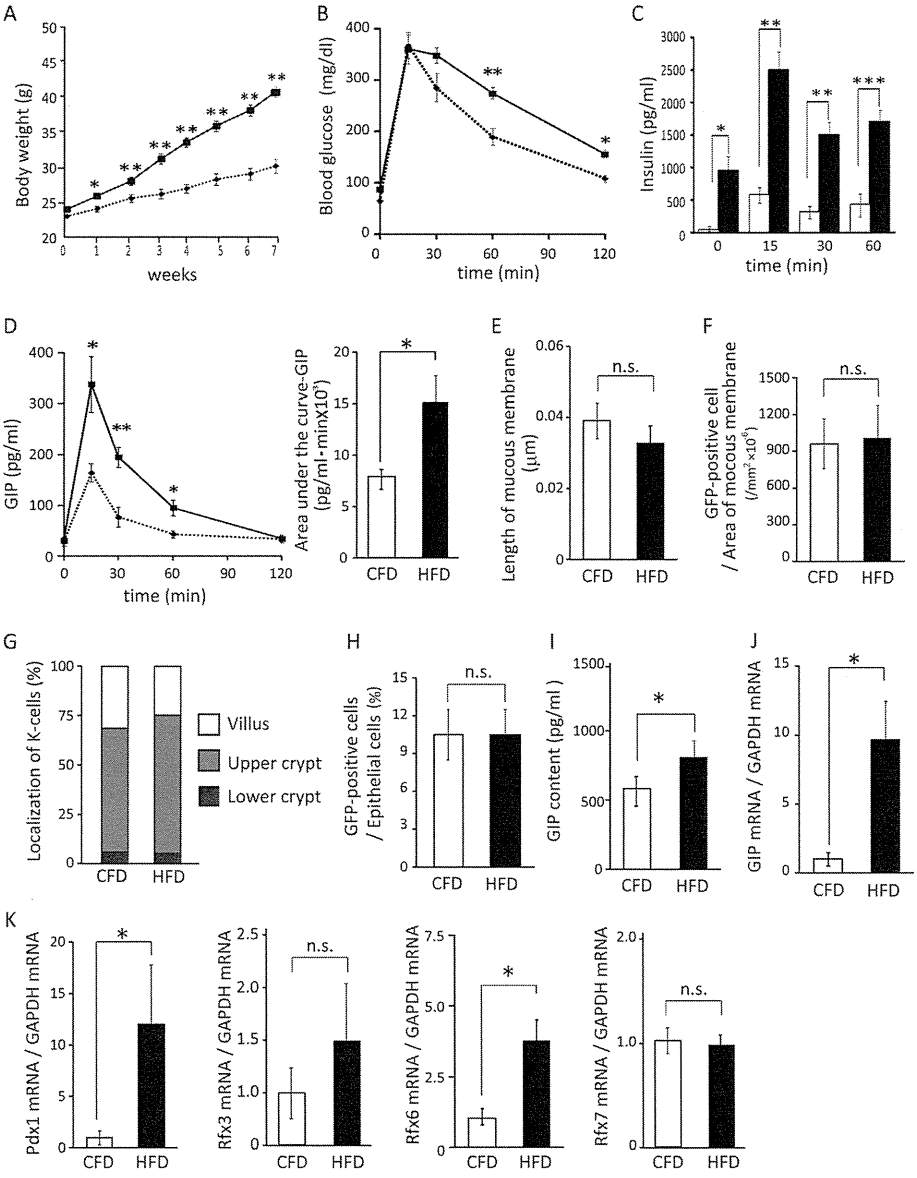

FIGURE 5. **Analysis of K-cells in the small intestine of CFD- and HFD-fed GIP-GFP heterozygous mice (histology, flow cytometry analysis, and gene expression).** *A*, body weight change of CFD-fed (*dashed line*) and HFD-fed (*continuous line*) GIP-GFP heterozygous mice (n = 5–7). *B–D*, blood glucose (*B*), insulin (*C*), and GIP levels (*D*) during OGTT after 8 weeks of CFD- or HFD-feeding (n = 5). *Dashed line* and *white box* shows CFD group, and *continuous line* and *black box* shows CFD group. *, $p \leq 0.05$; **, $p \leq 0.01$; ***, $p \leq 0.001$ *versus* CFD-fed mice. *E*, length of mucous membrane in upper small intestine (n = 5). *F*, number of GFP-positive cells by immunohistochemistry (n = 5). *G*, localization of K-cells in the upper small intestine by immunohistochemistry (n = 5). *H*, number of K-cells in the upper small intestine by flow cytometry analysis (n = 5). *I*, GIP content in upper small intestine (n = 5–7). *J*, GIP mRNA levels in GFP-positive cells (n = 8–10). *K*, Pdx1, Rfx3, Rfx6, and Rfx7 mRNA levels in GFP-positive cells (n = 8–10). *, $p \leq 0.05$; *n.s.*, not significant.

which regulates the *gip* promoter activity. Furthermore, Rfx6 was overexpressed in STC-1 cells by transfection of Rfx6 expression plasmids. The expression levels of Rfx6 mRNA levels were significantly higher in Rfx6-overexpressing cells compared with control (Fig. 4*E*). Rfx6 had no effect on the expression levels of to Pdx1 mRNA. GIP mRNA expression levels were significantly increased in Rfx6-overexpressing cells, but GLP-1 mRNA expression levels were not (Fig. 4*F*).

HFD Feeding Increases GIP Secretion and Induces Obesity and Insulin Hypersecretion in GIP-GFP Heterozygous Mice—To investigate the mechanisms of GIP hypersecretion in HFD-induced obesity *in vivo*, GIP-GFP heterozygous mice were fed CFD or HFD for 8 weeks. One week after starting these diets, the body weight of the HFD group was significantly increased compared with that of the CFD group (Fig. 5*A*). There was no difference in food and water intake between the CFD and HFD groups (data not shown). After CHD or HFD feeding for 8 weeks, OGTTs were performed. Blood glucose levels were significantly increased at 60 and 120 min during OGTT in HFD group (Fig. 5*B*). Insulin levels also were significantly increased in the HFD group (Fig. 5*C*). Insulin secretion (area under the curve-insulin) of the HFD group was increased about 5.5-fold compared with that of the CFD group (CFD group (n = 6) 38,221 ± 238 *versus* HFD group (n = 6) 211,835 ± 456; $p \leq$

0.001). GIP concentrations of HFD group at 15, 30, and 60 min were increased significantly compared with those of the CFD group (Fig. 5*D*). GIP secretion (area under the curve-GIP) of the HFD group was increased about 1.5-fold compared with that of the CFD group (CFD group ($n = 6$) 7368 ± 123 *versus* HFD group ($n = 6$) 10,531 ± 216; $p \leq 0.05$) These results show that HFD feeding increases GIP secretion and induces obesity and insulin hypersecretion in GIP-GFP heterozygous mice, which have only one normal *gip* gene.

GIP Hypersecretion in HFD-induced Obese Mice Is Not Due to Increase of K-cell Number but to Increase of GIP Expression in K-cells—To determine whether GIP hypersecretion involves an increased number of K-cells in HFD-fed GIP-GFP heterozygous mice, the number and localization of the K-cells in the upper small intestine were estimated and compared. The length of the mucous membrane and the number and localization of K-cells examined by immunohistochemistry were similar in the CFD and HFD group (Fig. 5, *E–G*). Flow cytometry analysis also showed no difference in K-cell number between the two groups (Fig. 5*H*). However, GIP content in the upper small intestine was significantly increased in the HFD group compared with that in the CFD group (Fig. 5*I*). In addition, in K-cells purified using flow cytometry, the expression levels of GIP mRNA were almost 10-fold higher in the HFD group than those in the CFD group (Fig. 5*J*). These results demonstrate that GIP hypersecretion under HFD-induced obesity is not due to an increase in K-cell number but to an increase of GIP mRNA expression and content in K-cells.

Rfx6 and Pdx1 mRNA Levels Were Increased in K-cells of HFD-induced Obese Mice—We also assessed the expression of other candidate genes in K-cells (GFP-positive cells) (Fig. 5*K*) and non-K-cells (GFP-negative cells). Both Rfx6 and Pdx1 mRNA levels were increased in K-cells of the HFD group compared with those in K-cells of the CFD group, but the mRNA expression levels of Rfx3 and Rfx7 were not. Other Rfx transcriptional factors (Rfx1, -2, -4, and -5) were not detected in the K-cells of HFD-fed mice. Furthermore, none of the Rfx transcriptional factors were detected in non-K-cells. Pdx1 mRNA expression was detected in non-K-cells, but there was no significant difference in the expression level between the CHD group and the HFD group (ratio of Pdx1 mRNA to GAPDH mRNA: CFD group ($n = 8$) 0.47 ± 0.15 *versus* HFD group ($n = 8$) 0.26 ± 0.08; $p = 0.24$). These results strongly suggest that an increase in Rfx6 expression as well as Pdx1 expression in K-cells stimulates GIP mRNA expression and content in K-cells of HFD-fed obese mice.

DISCUSSION

Analysis of K-cells *in vivo* has been impossible due to the inability to isolate the GIP-producing K-cells from intestinal epithelium. In this study, GIP-GFP mice enabled sorting GFP-positive cells as K-cells and revealed that the transcription factor Rfx6 is expressed exclusively in K-cells by microarray analysis and RT-PCR (Fig. 2*B*). Rfx3 and Rfx7 also were detected in K-cells by RT-PCR, but there were no significant differences in their expression between K-cells and non-K-cells (Fig. 2*B*). The *rfx* gene family of transcription factors was first detected in mammals as regulatory factors that bind to the promoter regions of major histocompatibility complex (*MHC*) class II genes (21); seven types of Rfx (Rfx1–7) have so far been identified. All Rfx transcription factors have a winged helix DNA binding domain. Rfx1–4 and -6 have a dimerization domain (22, 23), and Rfx6 forms homodimers or heterodimers with Rfx2 or Rfx3 (24, 25). Rfx6 was initially isolated from human genome sequences in 2008 (22). Serial Analysis of Gene Expression (SAGE) frequency data showed high expression of Rfx6 mRNA in the pancreas, liver, and heart, and RT-PCR analysis showed high expression of Rfx6 mRNA in human pancreas and intestine (20). However, it is known that Rfx3 mRNA is expressed in brain, placenta, pancreas, and pituitary and that Rfx3 directly regulates the promoters of *glut2* and glucokinase in pancreatic β-cells (26). Rfx7 is known to be expressed in many different tissues. *rfx3*- and *rfx6*-deficient mice were generated previously, and none of the endocrine cells, excluding pancreatic polypeptide-expressing cells, are detected in the islets of these mice (20, 27). These results suggest that Rfx3 and Rfx6 play a critical role in generating the endocrine cells in islets, but it is unknown whether they are associated with generation of enteroendocrine cells such as K-cells and L-cells. We examined incretin mRNA expression and content under the inhibition of Rfx6 expression in STC-1 cells. Other incretin GLP-1 mRNA expression and content were preserved in Rfx6-knockdown STC-1 cells. However, GIP mRNA expression and content were significantly decreased in the cells (Fig. 2, *E–G*). In addition, Rfx3 expression tended to be higher in GFP-positive cells than that in GFP-negative cells (Fig. 2*B*), but GIP mRNA expression, content, and secretion were not changed in Rfx3-knockdown STC-1 cells (data not shown). These results suggest that Rfx6 expressed exclusively in K-cells plays an important role in GIP expression, cellular content, and secretion in K-cells. In addition, we examined the effect of Rfx6 on the *gip* gene and found that Rfx6 binds to the region 5216–6512 bp upstream of the *gip* promoter gene (Fig. 4*D*) and that Rfx6 increased GIP mRNA expression in STC-1 cells (Fig. 4*F*). Further study is needed to clarify the regulatory mechanism of *gip* promoter activity by Rfx6. In previous studies, characterization of K-cells and microarray analysis were done using purified K-cells from the intestine of transgenic mice expressing a yellow fluorescent protein (YFP) under the control of the 200-kb rat *gip* promoter (28, 29), but Rfx6 expression in K-cells was not reported. The reason such a long promoter is required for specific expression of YFP in K-cells is not known, but it suggests that regulation of *gip* gene expression is under complex control. In this study, we established GIP-GFP mice in which GFP is under an endogenous native promoter. Using these GIP-GFP mice, we were able to determine that Rfx6 is expressed exclusively in K-cells.

In previous studies, Pdx1 expression was detected in K-cells, and *pdx1*-deficient mice showed a greatly decreased number of GIP-expressing cells in the intestine (18, 19). It also has been reported that Pdx1 binds 150 bp upstream of the *gip* promoter, activates the *gip* promoter in STC-1 cells, and that Pdx1 expression is essential for producing GIP in K-cells (18, 19). We found that there was no significant difference in Pdx1 mRNA expression between upper small intestinal K-cells and non-K-cells (Fig. 3*A*). These findings suggest the possibility that Rfx6 spe-

cifically expressed in K-cells plays a critical role in differentiation and GIP production of K-cells in collaboration with Pdx1. It was reported that Rfx6 mRNA expression is regulated by transcription factor neurogenin 3 (Ngn3) in the pancreas of the mouse fetus (30). In another report, no colocalization of Pdx1-expressing cells and Rfx6-expressing cells was found in pancreas of the mouse fetus using immunohistochemistry analysis, and Pdx-1 expression was decreased in the pancreas of Rfx6-deficient mice (20). In this study, Pdx1 mRNA expression levels were changed not only in Rfx6-knockdown STC-1 cells but also in Rfx6-overexpressing STC-1 cells, whereas Rfx6 expression levels were significantly decreased in Pdx1 knockdown STC-1 cells (Figs. 2*E*, 3*C*, and 4*E*). These results suggest that Rfx6 expression is regulated at least in part by Pdx1.

Increased blood GIP levels in obesity have been reported in several studies (7, 14–16). There is a report that healthy human subjects administered high fat food for 2 weeks showed increased plasma GIP levels without developing obesity, suggesting that GIP hypersecretion precedes obesity (31). GIP is released from K-cells into the circulation in response to various nutrients (32–34). Measurement of total GIP and total GLP-1 levels in humans challenged with glucose or meal shows that the postprandial plasma GIP level is greatly augmented when a meal containing abundant fat rather than simple glucose is consumed (35, 36). This suggests that intake of HFD increases GIP secretion and strengthens both direct and indirect effects of GIP on energy accumulation in adipose tissue. We previously reported that both GIP levels after glucose loading and body mass index have a positive correlation in healthy subjects (37). In this study, GIP levels during OGTT were increased in obese GIP-GFP heterozygous mice compared with those in lean GIP-GFP heterozygous mice, even though GIP-GFP heterozygous mice have only one normal *gip* gene, indicating these mice represent a useful model for analysis of the mechanisms involved in the augmented GIP secretion in HFD-induced obesity. A previous study reported that augmentation of GIP secretion in HFD feeding conditions is due to increased K-cell number (38). In that report, agglomerates of Pdx1 and GIP double-expressing cells were found inside the duodenal mucosa of obese rats after HFD feeding. In this study, however, we could not detect agglomerates of K-cells or an increase of K-cell number in the duodenum or upper small intestine of HFD-fed GIP-GFP heterozygous mice by immunohistochemistry and flow cytometry analysis. The reason for this discrepancy could be the difference of species, food composition, and/or duration of the HFD feeding period. In our study, GIP content was significantly increased in the upper small intestine of HFD-fed mice compared with that in CFD-fed mice, and GIP mRNA expression was increased in K-cells of HFD-fed mice. These results suggest that GIP hypersecretion in HFD-induced obese mice is due to increased GIP expression in K-cells. In this condition, the expression levels of Rfx6 and Pdx1 mRNA were significantly increased in K-cells (Fig. 5*K*). As Rfx6 and Pdx1 were found to be important transcriptional factors in producing GIP in K-cells in our results using Rfx6 knockdown and overexpression and in previous *in vitro* studies for Pdx1, an increase in Rfx6 and Pdx1 expressions might well be involved in GIP hypersecretion in K-cells in HFD-induced obese mice.

In conclusion, gene analysis of K-cells isolated from GIP-GFP mice enables identification of the transcription factor Rfx6 that is expressed exclusively in K-cells and is involved in the regulation of GIP expression. We also show that expression of Rfx6 and Pdx1 is up-regulated in the K-cells of HFD-induced obese mice, which suggests that induction of Rfx6 as well as Pdx1 plays a critical role in GIP hypersecretion in HFD-induced obesity.

Acknowledgments—We thank Prof. Douglas Hanahan, University of California, San Francisco, for kindly providing the STC-1 cells. We also thank Dr. Yoshitaka Hayashi, Research Institute of Environmental Medicine, Nagoya University, for helpful suggestions regarding the study. Mouse anti-GIP antibody was kindly provided by Merck Millipore.

REFERENCES

1. Reaven, G. M. (1988) Banting lecture 1988. Role of insulin resistance in human disease. *Diabetes* **37,** 1595–1607
2. Kahn, B. B., and Flier, J. S. (2000) Obesity and insulin resistance. *J. Clin. Invest.* **106,** 473–481
3. Lemieux, I., Pascot, A., Couillard, C., Lamarche, B., Tchernof, A., Alméras, N., Bergeron, J., Gaudet, D., Tremblay, G., Prud'homme, D., Nadeau, A., and Després, J. P. (2000) Hypertriglyceridemic waist. A marker of the atherogenic metabolic triad (hyperinsulinemia; hyperapolipoprotein B; small, dense LDL) in men? *Circulation* **102,** 179–184
4. Pederson, R. A. (1994) in *Gut Peptides: Biochemistry and Physiology* (Walsh, J. H., and Dockray, G. J., eds) pp. 217–259, Raven Press, New York
5. Drucker, D. J. (1998) Glucagon-like peptides. *Diabetes* **47,** 159–169
6. Seino, Y., Fukushima, M., and Yabe, D. (2010) GIP and GLP-1, the two incretin hormone. Similarities and difference. *J. Diabetes Invest.* **1,** 8–23
7. Miyawaki, K., Yamada, Y., Ban, N., Ihara, Y., Tsukiyama, K., Zhou, H., Fujimoto, S., Oku, A., Tsuda, K., Toyokuni, S., Hiai, H., Mizunoya, W., Fushiki, T., Holst, J. J., Makino, M., Tashita, A., Kobara, Y., Tsubamoto, Y., Jinnouchi, T., Jomori, T., and Seino, Y. (2002) Inhibition of gastric inhibitory polypeptide signaling prevents obesity. *Nat. Med.* **8,** 738–742
8. Tsukiyama, K., Yamada, Y., Yamada, C., Harada, N., Kawasaki, Y., Ogura, M., Bessho, K., Li, M., Amizuka, N., Sato, M., Udagawa, N., Takahashi, N., Tanaka, K., Oiso, Y., and Seino, Y. (2006) Gastric inhibitory polypeptide as an endogenous factor promoting new bone formation following food ingestion. *Mol. Endocrinol.* **20,** 1644–1651
9. Miyawaki, K., Yamada, Y., Yano, H., Niwa, H., Ban, N., Ihara, Y., Kubota, A., Fujimoto, S., Kajikawa, M., Kuroe, A., Tsuda, K., Hashimoto, H., Yamashita, T., Jomori, T., Tashiro, F., Miyazaki, J., and Seino, Y. (1999) Glucose intolerance caused by a defect in the entero-insular axis. A study in gastric inhibitory polypeptide receptor knockout mice. *Proc. Natl. Acad. Sci. U.S.A.* **96,** 14843–14847
10. Harada, N., Yamada, Y., Tsukiyama, K., Yamada, C., Nakamura, Y., Mukai, E., Hamasaki, A., Liu, X., Toyoda, K., Seino, Y., and Inagaki, N. (2008) A novel GIP receptor splice variant influences GIP sensitivity of pancreatic beta-cells in obese mice. *Am. J. Physiol. Endocrinol. Metab.* **294,** E61–E68
11. Usdin, T. B., Mezey, E., Button, D. C., Brownstein, M. J., and Bonner, T. I. (1993) Gastric inhibitory polypeptide receptor, a member of the secretin-vasoactive intestinal peptide receptor family, is widely distributed in peripheral organs and the brain. *Endocrinology* **133,** 2861–2870
12. Hauner, H., Glatting, G., Kaminska, D., and Pfeiffer, E. F. (1988) Effects of gastric inhibitory polypeptide on glucose and lipid metabolism of isolated rat adipocytes. *Ann. Nutr. Metab.* **32,** 282–288
13. Song, D. H., Getty-Kaushik, L., Tseng, E., Simon, J., Corkey, B. E., and Wolfe, M. M. (2007) Glucose-dependent insulinotropic polypeptide enhances adipocyte development and glucose uptake in part through Akt activation. *Gastroenterology* **133,** 1796–1805
14. Bailey, C. J., Flatt, P. R., Kwasowski, P., Powell, C. J., and Marks, V. (1986) Immunoreactive gastric inhibitory polypeptide and K cell hyperplasia in

obese hyperglycaemic (ob/ob) mice fed high fat and high carbohydrate cafeteria diets. *Acta Endocrinol.* **112,** 224–229
15. Flatt, P. R., Bailey, C. J., Kwasowski, P., Swanston-Flatt, S. K., and Marks, V. (1983) Abnormalities of GIP in spontaneous syndromes of obesity and diabetes in mice. *Diabetes* **32,** 433–435
16. Creutzfeldt, W., Ebert, R., Willms, B., Frerichs, H., and Brown, J. C. (1978) Gastric inhibitory polypeptide (GIP) and insulin in obesity. Increased response to stimulation and defective feedback control of serum levels. *Diabetologia* **14,** 15–24
17. Jonsson, J., Carlsson, L., Edlund, T., and Edlund, H. (1994) Insulin-promoter-factor 1 is required for pancreas development in mice. *Nature* **371,** 606–609
18. Jepeal, L. I., Fujitani, Y., Boylan, M. O., Wilson, C. N., Wright, C. V., and Wolfe, M. M. (2005) Cell-specific expression of glucose-dependent-insulinotropic polypeptide is regulated by the transcription factor PDX-1. *Endocrinology* **146,** 383–391
19. Fujita, Y., Chui, J. W., King, D. S., Zhang, T., Seufert, J., Pownall, S., Cheung, A. T., and Kieffer, T. J. (2008) Pax6 and Pdx1 are required for production of glucose-dependent insulinotropic polypeptide in proglucagon-expressing L cells. *Am. J. Physiol. Endocrinol Metab.* **295,** E648–E657
20. Smith, S. B., Qu, H. Q., Taleb, N., Kishimoto, N. Y., Scheel, D. W., Lu, Y., Patch, A. M., Grabs, R., Wang, J., Lynn, F. C., Miyatsuka, T., Mitchell, J., Seerke, R., Désir, J., Vanden Eijnden, S., Abramowicz, M., Kacet, N., Weill, J., Renard, M. E., Gentile, M., Hansen, I., Dewar, K., Hattersley, A. T., Wang, R., Wilson, M. E., Johnson, J. D., Polychronakos, C., and German, M. S. (2010) Rfx6 direct islet formation and insulin production in mice and humans. *Nature* **463,** 775–780
21. Reith, W., Barras, E., Satola, S., Kobr, M., Reinhart, D., Sanchez, C. H., and Mach, B. (1989) Cloning of the major histocompatibility complex class II promoter binding protein affected heredity defect in class II gene regulation. *Proc. Natl. Acad. Sci. U.S.A.* **86,** 4200–4204
22. Aftab, S., Semenec, L., Chu, J. S., and Chen, N. (2008) Identification and characterization of novel human tissue-specific RFX transcription factors. *BMC Evol. Biol.* **8,** 226–236
23. Katan-Khaykovich, Y., and Shaul, Y. (1998) RFX1, a single DNA-binding protein with a split dimerization domain, generates alternative complexes. *J. Biol. Chem.* **273,** 24504–24512
24. Rual, J. F., Venkatesan, K., Hao, T., Hirozane-Kishikawa, T., Dricot, A., Li, N., Berriz, G. F., Gibbons, F. D., Dreze, M., Ayivi-Guedehoussou, N., Klitgord, N., Simon, C., Boxem, M., Milstein, S., Rosenberg, J., Goldberg, D. S., Zhang, L. V., Wong, S. L., Franklin, G., Li, S., Albala, J. S., Lim, J., Fraughton, C., Llamosas, E., Cevik, S., Bex, C., Lamesch, P., Sikorski, R. S., Vandenhaute, J., Zoghbi, H. Y., Smolyar, A., Bosak, S., Sequerra, R., Doucette-Stamm, L., Cusick, M. E., Hill, D. E., Roth, F. P., and Vidal, M. (2005) Towarda proteome-scale map of the human protein-protein interaction network. *Nature* **437,** 1173–1178
25. Rhodes, D. R., Tomlins, S. A., Varambally, S., Mahavisno, V., Barrette, T., Kalyana-Sundaram, S., Ghosh, D., Pandey, A., and Chinnaiyan, A. M. (2005) Probabilistic model of the human protein-protein interaction network. *Nat. Biotechnol.* **23,** 951–959
26. Ait-Lounis, A., Bonal, C., Seguín-Estévez, Q., Schmid, C. D., Bucher, P., Herrera, P. L., Durand, B., Meda, P., and Reith, W. (2010) The transcription factor Rfx3 regulates beta-cell differentiation, function, and glucokinase expression. *Diabetes* **59,** 1674–1685
27. Ait-Lounis, A., Baas, D., Barras, E., Benadiba, C., Charollais, A., Nlend Nlend, R., Liègeois, D., Meda, P., Durand, B., and Reith, W. (2007) Novel function of ciliogenic transcription factor RFX3 in development of the endocrine pancreas. *Diabetes* **56,** 950–959
28. Parker, H. E., Habib, A. M., Rogers, G. J., Gribble, F. M., and Reimann, F. (2009) Nutrient-dependent secretion of glucose-dependent insulinotropic polypeptide from primary murine K cells. *Diabetologia* **52,** 289–298
29. Habib, A. M., Richards, P., Cairns, L. S., Rogers, G. J., Bannon, C. A., Parker, H. E., Morley, T. C., Yeo, G. S., Reimann, F., and Gribble, F. M. (2012) Overlap of endocrine hormone expression in the mouse intestine revealed by transcriptional profiling and flow cytometry. *Endocrinology* **153,** 3054–3065
30. Soyer, J., Flasse, L., Raffelsberger, W., Beucher, A., Orvain, C., Peers, B., Ravassard, P., Vermot, J., Voz, M. L., Mellitzer, G., and Gradwohl, G. (2010) Rfx6 is an Ngn3-dependent winged helix transcription factor required for pancreatic islet cell development. *Development* **137,** 203–212
31. Brøns, C., Jensen, C. B., Storgaard, H., Hiscock, N. J., White, A., Appel, J. S., Jacobsen, S., Nilsson, E., Larsen, C. M., Astrup, A., Quistorff, B., and Vaag, A. (2009) Impact of short-term high fat feeding on glucose and insulin metabolism in young healthy men. *J. Physiol.* **587,** 2387–2397
32. Yoder, S. M., Yang, Q., Kindel, T. L., and Tso, P. (2010) Differential responses of the incretin hormones GIP and GLP-1 to increasing doses of dietary carbohydrate but not dietary protein in lean rats. *Am. J. Physiol. Gastrointest. Liver Physiol.* **299,** G476–G485
33. Brown, J. C., Dryburgh, J. R., Ross, S. A., and Dupré, J. (1975) Identification and actions of gastric inhibitory polypeptide. *Recent Prog. Horm. Res.* **31,** 487–532
34. Falko, J. M., Crockett, S. E., Cataland, S., and Mazzaferri, E. L. (1975) Gastric inhibitory polypeptide (GIP) stimulated by fat ingestion in man. *J. Clin. Endocrinol. Metab.* **41,** 260–265
35. Vollmer, K., Holst, J. J., Baller, B., Ellrichmann, M., Nauck, M. A., Schmidt, W. E, and Meier, J. J. (2008) Predictors of incretin concentrations in subjects with normal, impaired, and diabetic glucose tolerance. *Diabetes* **57,** 678–687
36. Yamane, S., Harada, N., Hamasaki, A., Muraoka, A., Joo, E., Suzuki, K., Nasteska, D., Tanaka, D., Ogura, M., Harashima, S., and Inagaki, N. (2012) Effects of glucose and meal ingestion on incretin secretion in Japanese subjects with normal glucose tolerance. *J. Diabetes Invest.* **3,** 81–85
37. Harada, N., Hamasaki, A., Yamane, S., Muraoka, A., Joo, E., Fujita, K., and Inagaki, N. (2011) Plasma GIP and GLP-1 levels are associated with distinct factors after glucose loading in Japanese subjects. *J. Diabetes Invest.* **2,** 193–199
38. Gniuli, D., Calcagno, A., Dalla Libera, L., Calvani, R., Leccesi, L., Caristo, M. E., Vettor, R., Castagneto, M., Ghirlanda, G., and Mingrone, G. (2010) High-fat feeding stimulates endocrine, glucose-dependent insulinotropic polypeptide (GIP)-expressing cell hyperplasia in the duodenum of Wistar rats. *Diabetologia* **53,** 2233–2240

Efficacy and Safety of Switching from Basal Insulin to Sitagliptin in Japanese Type 2 Diabetes Patients

Authors
S.-I. Harashima[1], D. Tanaka[1], S. Yamane[1], M. Ogura[1], Y. Fujita[1], Y. Murata[2], M. Seike[2], T. Koizumi[2], M. Aono[2], Y. Wang[1], N. Inagaki[1]

Affiliations
[1] Department of Diabetes and Clinical Nutrition, Graduate School of Medicine, Kyoto University, Kyoto, Japan
[2] Department of Internal Medicine, Takashima General Hospital, Takashima, Japan

Key words
- sitagliptin
- basal insulin
- insulin secretion capacity

Abstract

Basal-supported oral therapy (BOT) is often used to treat poorly controlled type 2 diabetes. However, patients sometimes experience nocturnal and early morning hypoglycemia. Thus, maintaining targeted glycemic control by BOT is limited in some patients. We assessed the efficacy and safety of replacing basal insulin by sitagliptin therapy in Japanese type 2 diabetes patients on BOT. Forty-nine subjects were sequentially recruited for the 52-week, prospective, single arm study. Patients on BOT therapy were switched from basal insulin to sitagliptin. The primary endpoint was change in HbA1c in 52 weeks. The secondary endpoints were dropout rate, changes in body weight, frequency of hypoglycemia, and relationship between change in HbA1c and insulin secretion capacity evaluated by glucagon loading test. The average dose of basal insulin was 15.0±8.4 units. Sixteen subjects (31.3%) were dropped because replacement by sitagliptin was less effective for glycemic control. In these subjects, diabetes duration was longer, FPG and HbA1c at baseline were higher, and insulin secretion capacity was lower. Change in HbA1c in 52 weeks was −4 mmol/mol (95% CI −5 to −4 mmol/mol) ($p<0.05$). Change in body weight was −0.71 kg (95% CI −1.42 to −0.004 kg) ($p<0.05$). Frequency of hypoglycemia was decreased from 1.21±1.05 to 0.06±0.24 times/month. HbA1c level was improved if C-peptide index (CPI) was over 1.19. In conclusion, basal insulin in BOT can be replaced by sitagliptin with a decrease in HbA1c level and frequency of hypoglycemia in cases where insulin secretion capacity was sufficiently preserved.

received 29.05.2012
accepted 13.08.2012

Bibliography
DOI http://dx.doi.org/10.1055/s-0032-1323763
Published online: September 12, 2012
Horm Metab Res 2013; 45: 231–238

ISSN 0018-5043

Correspondence
S.-I. Harashima MD, PhD
Department of Diabetes and Clinical Nutrition
Graduate School of Medicine
Kyoto University
Kyoto 606-8507
Japan
Tel.: +81/75/751 3560
Fax: +81/75/771 6601
harasima@metab.kuhp.kyoto-u.ac.jp

Introduction

Basal insulin preparation is recommended by the American Diabetes Association (ADA)/European Association for the Study of Diabetes (EASD) consensus algorithm when lifestyle interventions and oral glucose-lowering agents no longer achieve the glycemic goal of hemoglobin A1c (HbA1c) level less than 53 mmol/mol [1,2]. Recently, 2 long-acting insulin analogues, insulin glargine and insulin detemir, are available that attain glycemic targets more effectively and safely [3,4]. There are no significant differences reported in glycemic control and overall hypoglycemia between the 2 analogues [5]. The combination of basal insulin and oral hypoglycemic agents (OHAs), known as basal-supported oral therapy (BOT), is often used to treat poorly controlled type 2 diabetes [6,7]. Better glycemic control, fewer hypoglycemic episodes, and less weight gain are obtained by BOT than by biphasic insulin [8]. In addition, BOT is relatively cost effective with the same glycemic control level as biphasic insulin regimen [9]. BOT is also helpful in Japanese type 2 diabetes patients. In the ALOHA (Add-on to Lantus® to OHA) study, in which 5223 Japanese type 2 diabetes patents participated, mean HbA1c was reduced from 75±13 to 60±13 mmol/mol in 24 weeks [10]. Although BOT is well-tolerated and effective for glycemic control, patients sometimes experience nocturnal and early morning hypoglycemia. In the ALOHA study, 0.97% of the patients experienced frequent hypoglycemia. In the 4 T-study, 1.3% of BOT-treated patients experienced hypoglycemia with loss of consciousness [8]. Another problem of BOT is that postprandial glucose is high, although morning fasting blood glucose level is within normal range. An increase in dosage of basal insulin or sulfonyl ureas (SUs); which are most commonly administrated in BOT-treated Japanese patients, is not always effective, and can result in increased hypoglycemia. In Japanese interview forms, frequency of hypoglyc-

emia induced by SUs is reported to be 1.3–2.8%. Thus, maintaining targeted glycemic control by BOT is limited in some patients.

Dipeptidyl peptidase-4 (DDP-4) inhibitor is a newly developed OHA that prevents degradation of the incretin hormones, glucagon-like peptide-1, and gastric inhibitory polypeptide [11]. This compound stimulates glucose-dependent insulin secretion and suppresses glucagon release, and can improve both fasting and postprandial glucose levels. Four different DPP-4 inhibitors are available in Japan: sitagliptin, vildagliptin, alogliptin, and linagliptin. Of these, sitagliptin is most widely used, partly because it was the first approved DPP-4 inhibitor and the safety and efficacy are acceptable in Japanese clinical practice. Generally, sitagliptin is more effective for glycemic control in Japanese patients compared to Caucasian patients [12, 13]. Sitaglipitn is usually combined with low dosage of SUs in Japan, less than or equal to 2 mg/day of glimepiride and 40 mg/day of gliclazide, which is enough for glycemic control when combined with sitagliptin [14]. Patients also show improved glycemic control even if insulin secretion capacity is insufficient for oral therapy [14, 15]. The main pathophysiology of Japanese type 2 diabetes is impairment of insulin secretion [16, 17]. Insulin secretion capacity in Japanese populations is only about half of that in Caucasians [18]. Both decreased basal and early phase insulin secretion contribute more to Japanese type 2 diabetes [16], and insulin therapy is usually required in those with C-peptide index (CPI) lower than 0.8 [19]. However, basal insulin therapy is not always ideal in some patients because postprandial glucose is still high and preprandial glucose is low, which results in large fluctuations in blood glucose. On the other hand, DPP-4 inhibitor might nevertheless ameliorate decreased early phase insulin secretion. This encouraged us to consider whether basal insulin can be replaced with sitagliptin in type 2 diabetes patients treated with SUs and basal insulin in at least some BOT cases.

We show here that sitagliptin can be switched from basal insulin in patients with C-peptide index (CPI) and/or secretory unit of islet in transplantation (SUIT) equal to or larger than 1.19 and/or 36.4, respectively, with beneficial effects on glycemic control.

Materials and Methods

Study design and participants

This was a prospective, 52-week, single center, and single arm intervention study to evaluate the effects on glycemic control of replacement of basal insulin to sitagliptin in type 2 diabetes patients inadequately controlled with BOT. Outpatients of Takashima General Hospital were recruited consecutively for a sample size of 45 subjects. Inclusion criteria were: type 2 diabetes treated with basal insulin (insulin glargine or detemir) and SUs (glimepiride or gliclazide) ± metformin ± thiazolidinedione ± α-glucosidase inhibitors for more than 1 year; aged ≥ 20 years; HbA1c level ≥ 52 mmol/mol; no improvement in HbA1c ≥ 5 mmol/mol within 3 months in BOT; and a fasting C-peptide reactin (CPR) of > 0.5 ng/ml. Exclusion criteria were: type 1 diabetes; secondary diabetes; alcoholism; severe depression, or severe psychological condition; malignancy; and abnormal hemoglobinemia. The study protocol was approved by the Institutional Review Board of Takashima General Hospital, and registered at the University hospital Medical Information Network in Japan (UMIN000005499). Written informed consent was obtained from all subjects.

Procedures and intervention

The duration of the study was 52 weeks. Subjects were screened for eligibility and gave basic demographic information, medical history, and frequency of hypoglycemia. Within a month before changing therapy from basal insulin to sitagliptin, glucagon loading test was performed without any OHAs or basal insulin for more than 24 h to evaluate insulin secretion capacity. When basal insulin was replaced by sitagliptin, the dosage of glimepiride or gliclazide was decreased to equal to or less than 2.0 mg/day or 40 mg/day, respectively, to prevent increased hypoglycemia if the subjects had been treated with more than 2.0 mg/day glimepiride or 40 mg/day gliclazide. If the subjects had been treated with equal to or less than 2.0 mg/day of glimepride or 40 mg/day of gliclazide, that dosage of SUs was maintained. Metformin (Met) and thiazolidinedione (TZD) were continued without any changes during the study. α-Glucosidase inhibitors were discontinued. The dosage of SUs was changed depending on the frequency of hypoglycemic episodes and glycemic control level. Sitagliptin was started at 50 mg/day, the usual initial dosage in Japan, which was increased to 100 mg/day if the HbA1c level did not reach 52 mmol/mol, since titration to 100 mg/day is acceptable.

Measurements

The primary endpoint was the change in HbA1c in 52 weeks. The secondary endpoints were dropout rate due to lesser efficacy of replacement by sitagliptin of basal insulin on glycemic control, change in body weight in 52 weeks, change in body mass index (BMI) in 52 weeks, change in frequency of hypoglycemia in 52 weeks, adverse events, and the correlation between change in HbA1c at the 8th week and insulin secretion capacity or CPI or SUIT at baseline. HbA1c are expressed in mmol/mol according to the recommendation of IFCC. CPI was calculated by the formula: [100 × fasting CPR (ng/ml)]/[18 × FPG (mM)] [19]. SUIT index was calculated by the formula: [250 × fasting CPR (nM)]/[(FPG − 3.43) (mM)] [20]. Blood glucose and C-peptide level were measured before (0 min) and 6 min after intravenous administration of 1 mg glucagon.

Statistical analysis

Sample size was estimated to be 34 to detect a 4 mmol/mol change in HbA1c in 52 weeks with a power of 95%, alpha 0.05 2-tailed, beta 0.20, standardized effect size 0.7. To take the dropout rate of 30% into account, the aim was to include 45 subjects. IBM SPSS Statistics was used for analysis. Dependent samples Student's *t*-test was used to compare the means of HbA1c level, insulin secretion capacity, BMI, body weight, age, and diabetes duration of the subjects between baseline and 52th week. Person's product-moment correlation test was used to evaluate the relationship between change in HbA1c and insulin secretion capacity or CPI or SUIT. To evaluate cutoff values of diabetes duration, FPG, HbA1c, 0-min CPR, 6-min CPR, delta-CPR, CPI, SUIT, and receiver operating characteristics curve (ROC) analysis were used. Independent sample Student's *t*-test was used to compare the mean of change in HbA1c in 52 weeks between subjects treated with sitagliptin + glimepiride and sitagliptin + gliclazide. Dunnett analysis was used to compare change in HbA1c in 52 weeks among subjects treated with sitagliptin + SUs and sitagliptin + SUs + MET and sitagliptin + SUs + TZD. A p-value of < 0.05 was considered as statistically significant.

Results

Participants

Forty-nine patients were eligible and were consecutively enrolled in the study (◎ **Table 1**). Average age of subjects was 70.0±10.2 years; ratio of male was 60.8%; duration of diabetes was 14.3±8.2 years; average body weight was 62.3±10.4 kg; average BMI was 24.3±3.8 kg/m^2; and HbA1c was 64±9 mmol/mol. All subjects were treated with SUs; 17 subjects (34.7%) were treated with glimepiride (average dose 1.67±1.47 mg) and 32 (65.3%) were treated with gliclazide (average dose 33.8±12.0 mg). Average dosage of basal insulin analogues was 15.0±8.4 units. Glucagon loading test showed that 0-min CPR, 6-min CPR, CPI, and SUIT were 1.65±1.02 ng/ml, 3.37±1.98 ng/ml, 1.19±0.64, and 36.5±22.1, respectively. Sixteen subjects (32.6%) were dropped due to an increase in HbA1c in 8th week; 6 (29.4%) and 11 (34.4%) were dropped in glimepiride- and gliclazide-treated subjects, respectively (◎ **Table 2**). No subjects were dropped for other reasons. Thirty-three subjects completed the study.

HbA1c findings and dosage of SUs and sitagliptin

Therapy adherence was confirmed by certified diabetes educators (nurses) in the study. Adherence of BOT therapy and the switching therapy were almost 100% for both therapies (data not shown).

HbA1c level in 52 weeks in final subjects was significantly decreased from 61±8 to 57±8 mmol/mol ($p<0.01$) (◎ **Table 2**). Change in HbA1c in 52 weeks was −4 mmol/mol (95% CI; −5 to −4 mmol/mol) ($p<0.05$). HbA1c levels in 52 weeks in glimepiride-treated subjects (n=12) were significantly decreased from 63±9 mmol/mol to 55±9 mmol/mol ($p<0.01$). Change in HbA1c in 52 weeks was −8 mmol/mol (95% CI; −11 to −5 mmol/mol) ($p<0.05$). HbA1c levels in 52 weeks in gliclazide-treated subjects (n=21) were significantly decreased from 54±6 to 58±7 mmol/mol ($p<0.05$). Change in HbA1c in 52 weeks was −2 mmol/mol (95% CI; −4 to −0 mmol/mol) ($p<0.05$). There was a significant difference in change in HbA1c in 52 weeks between glimepiride-treated and gliclazide-treated subjects ($p<0.01$). The original dosages of glimepiride and gliclazide before the study were 1.58±0.93 mg/day and 38.2±14.0 mg/day, respectively; the initial dosages at the beginning of the study were significantly decreased to 0.96±0.40 mg/day and 24.8±8.7 mg/day, respectively ($p<0.05$); and the final dosages were significantly increased to 1.42±0.57 mg/day and 31.4±12.0 mg/day, respectively, compared to the initial dosages ($p<0.05$), and were almost equal to the original dosages (◎ **Table 2**). Final dosage of sitagliptin was 74.2±25.4 mg/day in all subjects; 70.8±25.7 mg/day

Subjects (n)	49	**Basal insulin**	15.0±8.4 Units
Age (years)	70.0±10.2	**Medications**	SU 100%
			Glimepiride 34.7%
			1.67±1.47 mg
			Gliclazide 65.3%
			33.8±12.0 mg
Male	60.8%		
Diabetes duration (years)	14.3±8.2		Metformin 22.4%
			636±131 mg
Complications	Nephropathy		Thiazolidinedione 16.3%
	61.2%		10.3±3.9 mg
	Retinopathy		α-Glucosidase inhibitors
	69.4%		8.1%
	Neuropathy	**Glucagon test**	1.65±1.02
	42.8%	0-min CPR (ng/ml)	
	Cardiovascular diseases 34.7%	6-min CPR (ng/ml)	3.37±1.98
Weight (kg)	62.3±10.4	Delta CPR (ng/ml)	1.72±1.23
BMI (kg/m^2)	24.3±3.8	**CPI**	1.19±0.64
HbA1c (mmol/mol)	64±8	**SUIT**	36.5±22.1

Table 1 Demographic and clinical features of subjects participating in the study.

Table 2 Changes in HbA1c, and dosages of SUs and sitagliptin in final subjects.

Subjects (n)	Dropout rate (%) (n)	HbA1c level baseline (mmol/mol)	HbA1c level 52nd week (%)	Change in HbA1c (mmol/mol) (95% CI)	Original dosage of SUs (mg)	Initial dosage of SUs (mg)	Final dosage of SUs (mg)	Final dosage of sitagliptin (mg)
Final 33	32.6% 16	61±7	57±7**	−4* (−5 to −4)	–	–	–	74.2±25.4
Glimepiride 12	29.4% 5	63±9	55±9**	−8* (−11 to −5)	1.58±0.93	0.96±0.40*	1.42±0.57*	70.8±25.7
Gliclazide 21	34.4% 11	60±6	58±7*	−2* (−4 to −0)	38.2±14.0	24.8±8.7*	31.4±12.0*	77.3±25.5
SUs 23	30.3% 10	60±7	56±7*	−4* (−6 to −2)	–	–	–	67.4±24.3
SUs+Met 7	36.4% 4	64±9	58±8	−6* (−10 to −2)	–	–	–	87.5±23.1
SUs+TZD 3	62.5% 5	65±6	63±5	−2* (−5 to −0)	–	–	–	100±0.0

*$p<0.05$, **$p<0.01$

in glimepiride-treated subjects; and 77.3±25.5 mg/day in gliclazide-treated subjects with no significant difference between the 2 groups.

Of 33 subjects who completed the study, 22 subjects were treated with sitagliptin and SUs, 6 subjects were treated with sitagliptin and SUs and MET, and 3 subjects were treated with sitagliptin and SUs and TZD; changes in HbA1c in 52 weeks were −4 mmol/mol (95% CI; −6 to −2 mmol/mol) ($p<0.05$), −6 mmol/mol (95% CI; −10 to −2 mmol/mol) ($p<0.05$), and −3 mmol/mol (95% CI; −0.5 to −0 mmol/mol) ($p<0.05$), respectively (◎ **Table 2**). However, there was no significant difference among the 3 groups.

Change in body weight, BMI, and frequency of hypoglycemia

Body weight in final subjects at baseline was 64.2±9.5 kg, and was decreased to 63.5±8.7 kg at 52nd week. Change in body weight in 52 weeks was −0.71 kg (95% CI; −1.42 to −0.004 kg) ($p<0.05$) (◎ **Table 3**). BMI at baseline was 24.8±3.6 kg/m^2, and decreased to 24.5±3.4 kg/m^2 at 52nd week. Change in BMI in 52 weeks was −0.27 kg/m^2 (95% CI; −0.54 to 0.004 kg/m^2) ($p>0.05$). Frequency of hypoglycemia at baseline was 1.21±1.05 times/month, and was significantly decreased to 0.06±0.24 times/month at 52nd week ($p<0.001$). Change in frequency in hypoglycemia in 52 weeks was −1.21 times/months (95% CI; −1.5 to −0.80 times/month) ($p<0.05$) (◎ **Table 3**). During the study, no severe hypoglycemia was noted. During the study, no other adverse events were observed after replacement of basal insulin with sitagliptin.

Differences in HbA1c findings in 8-week in the final and dropped subjects

Sixteen of 49 subjects recruited dropped out after 8 weeks due to increased HbA1c level. The remaining 33 subjects completed the study. HbA1c level at baseline (0-week) in final subjects was 61±8 mmol/mol, and was significantly decreased to

Table 3 Changes in weight, BMI, and frequency in hypoglycemia.

	Weight (kg)	BMI (kg/m^2)	Hypoglycemia (times/month)
0-week	64.2±9.5	24.8±3.6	1.21±1.05
52nd week	63.5±8.7	24.5±3.4	0.06±0.24***
Change	−0.71*	−0.27	−1.21*
(95% CI)	(−1.42 to −0.004)	(−0.54 to 0.004)	(−1.5 to −0.80)

*$p<0.05$, ***$p<0.001$

	Diabetes Duration (Years)	FPG (mM)	HbA1c (mmol/mol)	0-min CPR (ng/ml)	6-min CPR (ng/ml)	Delta CPR (ng/ml)	CPI	SUIT
Cut-off value	16.5	8.2	6.1	1.25	2.80	1.60	1.34	37.5
AUC	0.468	0.507	0.252	0.530	0.570	0.541	0.509	0.482
Specificity	0.600	0.600	0.800	0.800	0.800	0.800	0.600	0.600
Sensitivity	0.545	0.568	0.159	0.432	0.455	0.364	0.545	0.432

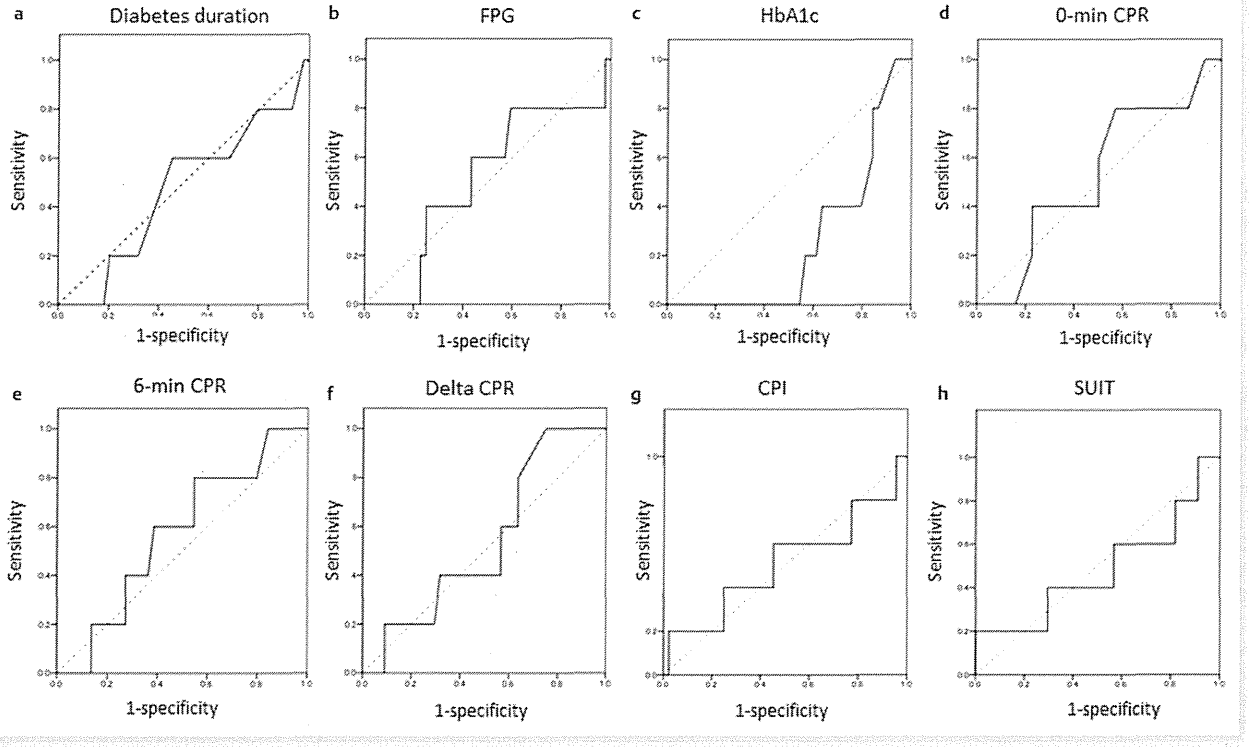

Fig. 1 Cutoff values and receiver-operator characteristic curves of **a** diabetes duration, **b** fasting plasma glucose, **c** HbA1c, **d** 0-min CPR, **e** 6-min CPR, **f** delta CPR, **g** CPI, and **h** SUIT at baseline. CPR: C-peptide reaction; CPI: C-peptide index; SUIT: the secretory unit of islet in transplantation.

Table 4 Changes in HbA1c and background of final and dropped subjects.

	Final subjects	Dropped subjects		Final subjects	Dropped subjects
	33	16		33	16
0 Wk HbA1c (mmol/mol)	61±7	69±10	**Original dosage of SUs (mg)**	Glimepiride 1.58±0.93 Gliclazide 36.2±10.2	Glimepiride 2.70±2.05 Gliclazide 38.2±14.1
8 Wk HbA1c (mmol/mol)	58±7***	73±10**	**Basal insulin (Units)**	14.8±9.3	15.2±6.4
Delta HbA1c (mmol/mol) (95% CI)	−4* (−5 to −2)	7* (0.3 to 11)	**FPG (mM)**	7.4±1.5	8.9±2.9*
Age (years)	69.8±10.7	70.5±9.3	**HbA1c (mmol/mol)**	61±7	69±10**
Male (%)	66.7	56.3	**Glucagon test** 0-min CPR (ng/ml)	1.95±1.25	1.37±0.64*
Diabetes duration (years)	12.1±6.6	18.7±9.5*	6-min CPR (ng/ml)	3.81±2.13	2.42±1.21*
Weight (kg)	64.2±9.5	58.4±11.5	Delta CPR (ng/ml)	1.98±1.35	1.16±0.69*
BMI (kg/m²)	24.8±3.6	23.4±4.0	**CPI**	1.35±0.68	0.92±0.51*
			SUIT	42.7±23.0	23.1±10.6**

*p<0.05, **p<0.01, ***p<0.001

58±7 mmol/mol at 8th week (p<0.001) (◎ **Table 4**). Change in HbA1c was −4 mmol/mol (95% CI; −5 to −2 mmol/mol) (p<0.05). On the other hand, HbA1c level at baseline (0-week) in dropped subjects was significantly higher than that in final subjects (p<0.05), and was significantly increased from 69±9 to 73±11 mmol/mol in 8 weeks (p<0.01). Change in HbA1c was +7 mmol/mol (95% CI; 0.3 to 11 mmol/mol) (p<0.05).

Differences in clinical factors in final and dropped subjects

There were no differences in age, sex, dosage of SUs, or dosage of basal insulin in final and dropped subjects (◎ **Table 4**). Body weight and BMI also were not significantly different (p=0.065 and p=0.2432, respectively). On the other hand, diabetes duration in dropped subjects was longer than that in final subjects (12.1±6.6 vs. 18.7±9.5 years, p<0.05). FPG and HbA1c also were higher in dropped subjects than in final subjects (FPG; 7.4±1.5 vs. 8.9±2.9 mM, p<0.05) (HbA1c; 61±7 vs. 69±9 mmol/mol, p<0.01).

Insulin secretion capacity was significantly higher in final subjects than that in dropped subjects (◎ **Table 4**) (p<0.05). In final subjects, CPR level at 0-min, 6-min, and delta CPR (6-min CPR to 0-min CPR) were 1.95±1.25 ng/ml, 3.81±2.13 ng/ml, and 1.98±1.35 ng/ml, respectively. In dropped subjects, CPR level at 0-min, 6-min, and delta CPR were 1.37±0.64 ng/ml, 2.42±1.21 ng/ml, and 1.16±0.69 ng/ml, respectively. CPI and SUIT index also were significantly higher in final subjects than those in dropped subjects. CPI at baseline in final subjects was 1.35±0.68, while that in dropped subjects was 0.92±0.51 (p<0.05). SUIT at baseline was 42.7±23.0 in final subjects, and 23.1±10.6 in dropped subjects (p<0.01). We examined cutoff values of diabetes duration, FPG, HbA1c, 0-min CPR, 6-min CPR, delta-CPR, CPI, and SUIT by analyzing ROC curves; they were 16.5 years, 8.2 mM, 62 mmol/mol, 1.25 ng/ml, 2.80 ng/ml, 1.60 ng/ml, 1.34, and 37.5, respectively (◎ **Fig. 1**).This indicates that with longer diabetes duration, insulin secretion capacity becomes lower and the consequent poorer glycemic control makes switching BOT-treated patients from basal insulin to sitagliptin unsafe.

Correlation between efficacy of sitagliptin on glycemic control and insulin secretion capacity, CPI, and SUIT

We examined whether or not insulin secretion capacity, CPI, or SUIT at baseline predicted the efficacy of replacing basal insulin with sitagliptin on glycemic control (◎ **Fig. 2**). There was a correlation between change in HbA1c at 8th week and 0-min CPR (r=−0.281), 6-min CPR (r=−0.326), and delta CPR (r=−0.290), assessed by glucagon loading test at baseline (◎ **Fig. 2a, b, c**) (p<0.05). In addition, CPI (r=−0.360) or SUIT (r=−0.306) at baseline was correlated with change in HbA1c at 8th week (◎ **Fig. 2d, e**) (p<0.05). The value of 0-min CPR, 6-min CPR, delta CPR, CPI, and SUIT at which the HbA1c level was not increased by replacement of basal insulin by sitagliptin were calculated to be 1.64 ng/ml, 3.36 ng/ml, 1.71 ng/ml, 1.19, and 36.4, respectively, by Pearson's product-moment correlation test (◎ **Table 5**). The value of 0-min CPR, 6-min CPR, delta CPR, CPI, and SUIT at which the HbA1c level was decreased by 0.5% in 8 weeks were calculated to be 1.86 ng/ml, 3.83 ng/ml, 1.98 ng/ml, 1.36, and 41.3, respectively. Other clinical characteristics of the patients such as disease duration and body weight were not significantly correlated with efficacy of replacing basal insulin with sitagliptin on glycemic control (data not shown).

Discussion

We show here that basal insulin can be switched to sitagliptin with good effects in type 2 diabetes patients treated with BOT. With this treatment, the HbA1c level decreased from 61±7 to 57±7 mmol/mol in 52-week (p<0.01). The change in HbA1c in 52 weeks was −4 mmol/mol (95% CI; −5 to −4 mmol/mol) (p<0.05). The efficacy of switching to sitagliptin from basal insulin was correlated with insulin secretion capacity, CPI, and SUIT; CPI being most correlated marker in the present study. The average CPI in final subjects was 1.35±0.68 ng/ml, while that of dropped subjects was 0.92±0.51 ng/ml. Pearson's product-moment correlation test revealed that HbA1c was improved by switching from basal insulin to sitagliptin if CPI was equal to or higher than 1.19 (◎ **Fig. 2d** and ◎ **Table 5**). Similarly, basal insulin could be switched to sitagliptin if SUIT was equal to or larger than 36.4 (◎ **Fig. 2e** and ◎ **Table 5**). In the dropped subjects, diabetes duration was longer, FPG and HbA1c were worse, 0-min CPR, 6-min CPR, delta-CPR, CPI, and SUIT were lower compared to those in final subjects (◎ **Table 4**). Cutoff values were 16.5 years, 8.2 mM, 62 mmol/mol, 1.25 ng/ml, 2.80 ng/ml, 1.60 ng/ml, 1.34, and 37.5, respectively (◎ **Fig. 1**). This suggests that the efficacy of switching from basal insulin to sitagliptin, when

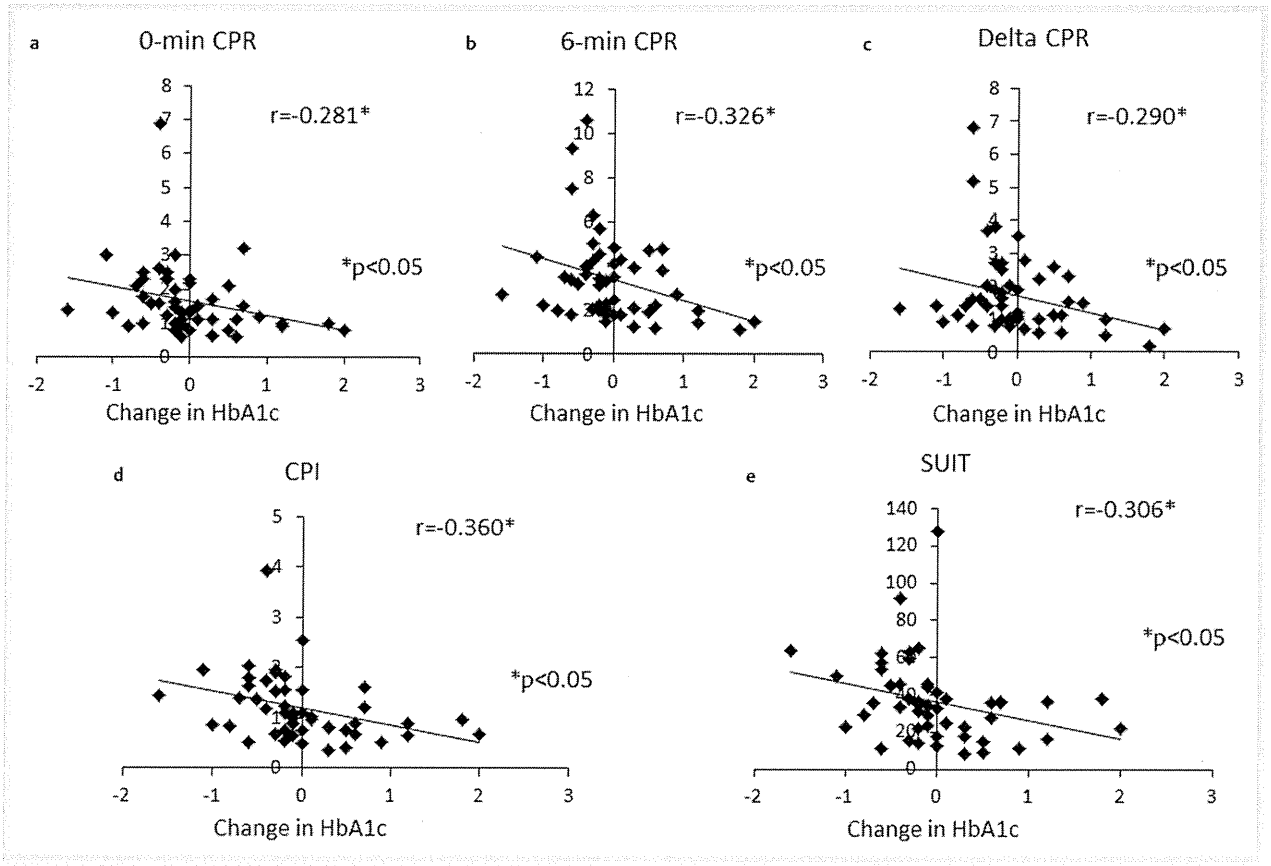

Fig. 2 Relationship between changes in HbA1c in 8 weeks and results of glucagon loading test, CPI, and SUIT at baseline. Changes in HbA1c in 8 weeks and 0-min CPR **a**, 6-min CPR **b**, delta CPR **c**, CPI **d**, and SUIT index **e** at baseline. CPR: C-peptide reaction; CPI: C-peptide index; SUIT: the secretory unit of islet in transplantation. *p<0.05.

Table 5 Correlation between change in HbA1c and insulin secretion capacity.

Change in HbA1c (mmol)	0-Minute CPR (ng/ml)	6-Minute CPR (ng/ml)	Delta CPR (ng/ml)	CPI	SUIT
0.0	1.64	3.36	1.71	1.19	36.4
−5	1.86	3.83	1.98	1.36	41.3

combined with SUs, is dependent on basal glycemic control and the insulin secretion capacity. Baseline HbA1c of dropped subjects was higher than that of the final subjects. A higher dosage of basal insulin was required to reach target HbA1c level in dropped subjects compared to that in final subjects because of lower insulin secretion capacity. Thus, if baseline HbA1c level were reduced by increasing the dosage of basal insulin, it would be difficult to replace basal insulin with sitagliptin.

Replacement of basal insulin by sitagliptin resulted in a reduction in body weight and hypoglycemia. Body weight was reduced by 0.71 kg (95% CI; −1.41 to −0.004 kg) ($p<0.05$). Frequency of hypoglycemia was decreased from 1.21±1.05 to 0.06±0.24 times/month ($p<0.001$). Since sitagliptin is known to be body weight neutral [21,22], discontinuation of basal insulin might contribute to body weight reduction. The combination of basal insulin and SUs often induces mild hypoglycemia by which patients feel a sense of hunger and eat between-meal snacks. This sometimes induces weight gain and poor glycemic control in BOT-treated patients. On the other hand, combination therapy with sitagliptin and low dosage SUs (less than or equal to 2 mg/day glimepiride or 40 mg/day gliclazide) was body weight neutral or led to a decrease in BMI [14]. In the current study, hypoglycemia seldom occurred, and BMI was significantly decreased by 0.38 kg/m^2 (95% CI −0.72 to −0.04 kg/m^2) [14]. Switching from basal insulin to sitagliptin also reduced the frequency of hypoglycemia. Although energy intake was not evaluated between baseline and 52-week in the present study, patients who had previously experienced frequent hypoglycemia reported to their physicians that the number of between-meal snacks in 52 weeks was fewer than at baseline. Thus, excess energy intake may be reduced after switching from basal insulin to sitagliptin to account for some of the body weight reduction and improvement in HbA1c. Another reason for improvement in the HbA1c level may be the reduced postprandial glucose level by the combination therapy with sitagliptin and SUs compared to that by BOT.

The combination therapy of glimepiride and sitagliptin was more effective for HbA1c reduction than that of gliclazide and sitagliptin. Recently, it was reported that cAMP sensor Epac2 is a direct target of several sulfonylureas [23]. Tolbutamide, glibenclimide, and glimepiride bound Epac2 and enhanced glucose-stimulated insulin secretion. However, gliclazide did not bind Epac2. Because Epac2 also mediates the potentiation of insulin secretion by cAMP increased by endogenous incretin, the combination therapy of glimepiride and sitagliptin enhances more insulin secretion through activation of Epac2. This might be a potential mechanism why the combination therapy of glimepir-

ide and sitagliptin was more effective for glycemic control than that of gliclazide and sitagliptin.

Generally, insulin secretion capacity of Japanese is as half as that of Caucasian [16–18]. Therefore, more than 60% of Japanese type 2 diabetes patients are treated with SUs [24]. DPP-4 inhibitor now is one of the most popular OADs, and more than 2 million patients were treated with DPP-4 inhibitors in Japan. Based on pathophysiology of Japanese patients and the mechanism of incretin effect, the combination therapy with SUs and DPP-4 inhibitors seems to be most effective for glycemic control compared to that with other OADs and DPP-4 inhibitors. On the other hand, the main pathophysiology of Caucasian type 2 diabetes is insulin resistance compared to that of Japanese type 2 diabetes [25,26]. Dosage of basal insulin in BOT in Caucasian patients is greater than that in Japanese patients. For example, in 4-T study, the mean dosage of basal insulin was 86 U (1.03 U/kg) [8], while 8.5 U (0.15 U/kg) in Japanese type 2 diabetes [10], and 15 U (0.24 U/kg) in our study. Therefore, it is not sure if basal insulin could be replaced with DPP-4 inhibitors even in subjects treated with high dosage of basal insulin. However, there is still a possibility that in Caucasian subjects whose BMI is less than 25 kg/m^2 and CPI is over 1.3, basal insulin could be replaced with DPP-4 inhibitors. Or, if the combination therapy with high dosage of MET and DPP-4 inhibitors is more effective for glycemic control compared to other combinations in Caucasian type 2 diabetes, basal insulin with MET could be replaced with DPP-4 inhibitors and metformin.

During the course of the disease, type 2 diabetes patients are treated with several OHAs [27,28]. However, if the HbA1c level does not reach less than 53 mmol/mol, insulin treatment is considered the next step [1,2]. BOT is often selected for outpatients because once daily injection is acceptable and the glycemic control is superior, with fewer hypoglycemic episodes and less weight gain compared to biphasic insulin [8]. In Japan, the commonly used SUs are combined with basal insulin in BOT [10]. One of the biggest problems of combination therapy with basal insulin and SUs is the high level of postprandial blood glucose while fasting blood glucose is within normal range. An increase in dosage of SUs or basal insulin does not resolve this problem, and sometimes leads to increased hypoglycemia. However, our results show that better glycemic control and lower frequency of hypoglycemia is obtained when switching from basal insulin to sitagliptin in subjects with sufficiently preserved insulin secretion capacity.

The advantages of discontinuation of basal insulin are 1) patients become free from daily injections; 2) they do not need to regularly perform self-monitoring of blood glucose (SMBG); and 3) oral therapy costs less than insulin therapy.

In summary, basal insulin in BOT can be switched to sitagliptin if CPI and/or SUIT are equal to or higher than 1.19 or 36.4, respectively. On the other hand, sitagliptin can be added to insulin therapy if insulin secretion capacity is not sufficient for switching to sitagliptin. However, the effectiveness of combination therapy with basal insulin and sitagliptin on glycemic control in type 2 patients with CPI and/or SUIT less than 1.19 or 36.4, respectively, is unknown. Further studies are required to determine the optimum insulin secretion capacities for switching BOT therapy to sitagliptin combined with SUs or combination therapy with sitagliptin and basal insulin or GLP-1 receptor analogues.

Acknowledgements

The study conception and protocol were by SH and NI. Patient examinations were by SH, TF, TK, and MA. Collection of data was by YW and MO. The statistical analysis was by DT, SY, and YF. The manuscript development was by Dr. SH and NI.

Conflict of Interest

None of the authors have any conflicts of interest to declare.

References

1 *Nathan DM, Buse JB, Davidson MB, Ferrannini E, Holman RR, Sherwin R, Zinman B; American Diabetes Association; European Association for Study of Diabetes.* Medical management of hyperglycemia in type 2 diabetes: a consensus algorithm for the initiation and adjustment of therapy: a consensus statement of the American Diabetes Association and the European Association for the Study of Diabetes. Diabetes Care 2009; 32: 193–203

2 *Nathan DM, Buse JB, Davidson MB, Ferrannini E, Holman RR, Sherwin R, Zinman B; American Diabetes Association; European Association for Study of Diabetes.* Medical management of hyperglycemia in type 2 diabetes mellitus: a consensus algorithm for the initiation and adjustment of therapy: a consensus statement from the American Diabetes Association and the European Association for the Study of Diabetes. Diabetologia 2009; 52: 17–30

3 *Heinemann L, Linkeschova R, Rave K, Hompesch B, Sedlak M, Heise T.* Time-action profile of the long-acting insulin analog insulin glargine (HOE901) in comparison with those of NPH insulin and placebo. Diabetes Care 2000; 23: 644–649

4 *Plank J, Bodenlenz M, Sinner F, Magnes C, Görzer E, Regittnig W, Endahl LA, Draeger E, Zdravkovic M, Pieber TR.* A double-blind, randomized, dose-response study investigating the pharmacodynamic and pharmacokinetic properties of the long-acting insulin analog detemir. Diabetes Care 2005; 28: 1107–1112

5 *Swinnen SG, Simon AC, Holleman F, Hoekstra JB, Devries JH.* Insulin detemir versus insulin glargine for type 2 diabetes mellitus. Cochrane Database Syst Rev 2011; 6: CD006383

6 *Blicklé JF, Hancu N, Piletic M, Profozic V, Shestakova M, Dain MP, Jacqueminet S, Grimaldi A.* Insulin glargine provides greater improvements in glycaemic control vs. intensifying lifestyle management for people with type 2 diabetes treated with OADs and 7–8% A1c levels. The TULIP study. Diabetes Obes Metab 2009; 11: 379–386

7 *Schreiber SA, Ferlinz K, Haak T.* The long-term efficacy of insulin glargine plus oral antidiabetic agents in a 32-month observational study of everyday clinical practice. Diabetes Technol Ther 2008; 10: 121–127

8 *Holman RR, Farmer AJ, Davies MJ, Levy JC, Darbyshire JL, Keenan JF, Paul SK; 4-T Study Group.* Three-year efficacy of complex insulin regimens in type 2 diabetes. N Engl J Med 2009; 361: 1736–1747

9 *Pfohl M, Dippel FW, Kostev K, Fuchs S, Kotowa W.* Different persistence on initial basal supported oral therapy in Type 2 diabetics is associated with unequal distributions of insulin treatment regimens under real-life conditions in Germany. Int J Clin Pharmacol Ther 2010; 48: 761–766

10 *Kadowaki T.* Analysis of ALOHA (add-on Lantus® to OHA) study: Basal supported oral therapy (BOT) with insulin glargine resulted in reduction of HbA1c, FPG and PPG with nearly 2% incidence of adverse drug reactions. Dubai: World Diabetes Congress, 2011

11 *Seino Y, Fukushima M, Yabe D.* GIP and GLP-1, two incretin hormones: Similarities and differences. J Diabetes Invest 2010; 1: 8–23

12 *Tajima N, Kadowaki T, Odawara M, Nishi M, Taniguchi T, Arjona Ferreira JC.* Addition of sitagliptin to ongoing glimepiride therapy in Japanese patients with type 2 diabetes over 52 weeks leads to improved glycemic control. Diabetol Int 2011; 2: 32–44

13 *Hermansen K, Kipnes M, Luo E, Fanurik D, Khatami H, Stein P.* Efficacy and safety of the dipeptidyl peptidase-4 inhibitor, sitagliptin, in patients with type 2 diabetes mellitus inadequately controlled on glimepiride alone or on glimepiride and metformin. Diabetes Obes Metab 2007; 9: 733–745

14 *Harashima SI, Ogura M, Tanaka D, Fukushima T, Wang Y, Koizumi T, Aono M, Murata Y, Seike M, Inagaki N.* Sitagliptin add-on to low dosage sulfonylureas: efficacy and safety of combination therapy on glycemic control and insulin secretion capacity in type 2 diabetes. Int J Clin Prac 2012; 66: 465–476
15 *Kubota A, Matsuba I, Saito T, Nabe K, Seino Y.* Secretory units of islets in transplantation index is a useful clinical marker to evaluate the efficacy of sitagliptin in treatment of type 2 diabetes mellitus. J Diabetes Invest 2011; 5: 377–380
16 *Fukushima M, Usami M, Ikeda M, Nakai Y, Taniguchi A, Matsuura T, Suzuki H, Kurose T, Yamada Y, Seino Y.* Insulin secretion and insulin sensitivity at different stages of glucose tolerance: a cross-sectional study of Japanese type 2 diabetes. Metabolism 2004; 53: 831–835
17 *Fukushima M, Suzuki H, Seino Y.* Insulin secretion capacity in the development from normal glucose tolerance to type 2 diabetes. Diabetes Res Clin Pract 2004; 66: S37–S47
18 *Abdul-Ghani MA, Matsuda M, Jani R, Jenkinson CP, Coletta DK, Kaku K, DeFronzo RA.* The relationship between fasting hyperglycemia and insulin secretion subjects with normal or impaired glucose tolerance. Am J Physiol Endocrinol Metab 2008; 295: E401–E406
19 *Funakoshi S, Fujimoto S, Hamasaki A, Fujiwara H, Fujita Y, Ikeda K, Hamamoto Y, Hosokawa M, Seino Y, Inagaki N.* Analysis of factors influencing pancreatic beta-cell function in Japanese patients with type 2 diabetes: Association with body mass index and duration of diabetic exposure. Diabetes Res Clin Pract 2008; 82: 353–358
20 *Yamada Y, Fukuda K, Fujimoto S, Hosokawa M, Tsukiyama K, Nagashima K, Fukushima M, Suzuki H, Toyoda K, Sassa M, Funakoshi S, Inagaki N, Taniguchi A, Sato TS, Matsumoto S, Tanaka K, Seino Y.* SUIT, secretory units of islets in transplantation: An index for therapeutic management of islet transplanted patients and its application to type 2 diabetes. Diabetes Res Clin Pract 2006; 74: 222–226
21 *Esposito K, Cozzolino D, Bellastella G, Maiorino MI, Chiodini P, Ceriello A, Giugliano D.* Dipeptidyl peptidase-4 inhibitors and HbA1c target of <7% in type 2 diabetes: meta-analysis of randomized controlled trials. Diabetes Obes Metab 2011; 13: 594–603
22 *Gallwitz B, Häring HU.* Future perspectives for insulinotropic agents in the treatment of type 2 diabetes-DPP-4 inhibitors and sulphonylureas. Diabetes Obes Metab 2010; 12: 1–11
23 *Zhang CL, Katoh M, Shibasaki T, Minami K, Sunaga Y, Takahashi T, Yokoi N, Iwasaki M, Miki T, Seino S.* The cAMP sensor Rpac2 is a direct target of antidiabetic sulfonylurea drugs. Science 2009; 25: 607–610
24 *Arai K, Matoba K, Hirao K, Matsuba I, Takai M, Takeda H, Kanamori A, Yamauchi M, Mori H, Terauchi Y.* Present status of sulfonylurea treatment for type 2 diabetes in Japan: second report of a cross-sectional survey of 15652 patients. Endocr J 2010; 57: 499–507
25 *Welch S, Gebhart SS, Bergman RN, Phillips LS.* Minimal model analysis of intravenous glucose tolerance test-derived insulin sensitivity in diabetic subjects. J Clin Endocrinol Metab 1990; 71: 1508–1518
26 *Taniguchi A, Nakai Y, Fukushima M, Kawamura H, Imura H, Nagata I, Tokuyama K.* Pathogenic factors responsible for glucose intolerance in patients with NIDDM. Diabetes 1992; 41: 1540–1546
27 *Tahrani AA, Bailey CJ, Del Prato S, Barnett AH.* Management of type 2 diabetes: new and future developments in treatment. Lancet 2011; 378: 182–197
28 *DeFronzo RA.* Current issues in the treatment of type 2 diabetes. Overview of newer agents: where treatment is going. Am J Med 2010; 123: S38–S48

Clinical and functional characterization of the Pro1198Leu *ABCC8* gene mutation associated with permanent neonatal diabetes mellitus

Tomoyuki Takagi[1], Hiroto Furuta[1]*, Masakazu Miyawaki[2], Kazuaki Nagashima[3], Takeshi Shimada[1], Asako Doi[1], Shohei Matsuno[1], Daisuke Tanaka[3], Masahiro Nishi[1], Hideyuki Sasaki[1], Nobuya Inagaki[3], Norishige Yoshikawa[2], Kishio Nanjo[4], Takashi Akamizu[1]

ABSTRACT

Aims/Introduction: The adenosine triphosphate (ATP)-sensitive potassium (K_{ATP}) channel is a key component of insulin secretion in pancreatic β-cells. Activating mutations in *ABCC8* encoding for the sulfonylurea receptor subunit of the K_{ATP} channel have been associated with the development of neonatal diabetes mellitus (NDM). The aim was to investigate clinical and functional characterization of the Pro1198Leu *ABCC8* gene mutation associated with permanent NDM (PNDM).

Materials and Methods: The coding regions and conserved splice sites of *KCNJ11*, *ABCC8* and *INS* were screened for mutations in a 12-year-old girl diagnosed with PNDM. The functional property of the mutant channel identified was examined with patch-clamp experiments in COS-1 cells. We also investigated the difference of effectiveness between two groups of oral sulfonylureas *in vitro* and in the patient.

Results: We identified a heterozygous missense mutation (c.3593 C>T, Pro1198Leu) in *ABCC8*. The mutated residue (P1198) is located within a putative binding site of sulfonylureas, such as tolbutamide or gliclazide. In patch-clamp experiments, the mutant channel was less ATP sensitive than the wild type. Furthermore, the sensitivity to tolbutamide was also reduced in the mutant channel. In addition to the tolbutamide/gliclazide binding site, glibenclamide is thought to also bind to another site. Glibenclamide was more effective than other sulfonylureas *in vitro* and in the patient. The treatment of the patient was finally able to be switched from insulin injection to oral glibenclamide.

Conclusions: We identified the Pro1198Leu *ABCC8* mutation in a PNDM patient, and clarified the functional and clinical characterization. The present findings provide new information for understanding PNDM. (J Diabetes Invest, doi: 10.1111/jdi.12049, 2013)

KEY WORDS: *ABCC8*, Neonatal diabetes, Sulfonylurea receptor

INTRODUCTION

Neonatal diabetes mellitus (NDM) is a specific form of diabetes[1]. It has been defined as diabetes with onset before 6 months-of-age and autoantibody negative for type 1 diabetes in general. NDM is classified into two categories clinically. One is transient NDM (TNDM), in which diabetes develops within the first few weeks of life and resolves by a few months of age, although it might frequently relapse in adolescence or young adulthood. The other is permanent NDM (PNDM), in which diabetes does not remit and the patients usually require insulin treatment for life. Approximately 50% of NDM is transient and 50% is permanent[2]. The majority (~70%) of cases of TNDM have abnormalities in the imprinted region of chromosome 6q24, such as paternal uniparental isodisomy, paternally inherited duplication and maternal methylation defects, leading to overexpression of paternally expressed genes[3]. The adenosine triphosphate (ATP)-sensitive potassium (K_{ATP}) channel is a key component of insulin secretion in pancreatic β-cells. The channel is comprised of two proteins, an inwardly rectifying potassium ion pore-forming subunit (Kir6.2; encoded by *KCNJ11*) and a high-affinity β-cell sulfonylurea receptor (SUR1; encoded by *ABCC8*)[4]. Activating mutations in *KCNJ11* and *ABCC8* account for 12% and 13% of cases of TNDM, respectively[5]. They also account for 31% and 10% of cases of PNDM, respectively[6]. Furthermore, 12% of PNDM is caused by mutations in the insulin (*INS*) gene itself[6]. It has also been reported that a few cases of PNDM are attributed to genetic abnormalities in other genes, such as *GCK, FOXP3, EIF2AK3, PDX1, PTF1A, GLIS3, NEUROD1* and *HNF1B*, which are important to pancreatic β-cell function and development[1].

The K_{ATP} channel plays a key role in glucose-dependent insulin secretion from pancreatic β-cells. After entry of glucose into

[1]First Department of Medicine and [2]Department of Pediatrics, Wakayama Medical University, [4]Wakayama Rosai Hospital, Wakayama, and [3]Department of Diabetes and Clinical Nutrition, Graduate School of Medicine, Kyoto University, Kyoto, Japan
*Corresponding author. Hiroto Furuta Tel.: +81-73-441-0625 Fax: +81-73-445-9436
E-mail address: hfuruta@wakayama-med.ac.jp
Received 29 October 2012; revised 15 November 2012; accepted 20 November 2012